Czech Technical University in Prague

Faculty of Nuclear Sciences
and Physical Engineering

Department of Physics

Spectra of Comb Graphs

BACHELOR'S THESIS

Author: Štěpán Timr

Supervisor: prof. RNDr. Pavel Exner, DrSc.

Academic year: 2010/2011

Acknowledgment

I would like to express my gratitude to prof. RNDr. Pavel Exner, DrSc., who kept giving my work its direction and was willing to spend his precious time discussing it with me. I would like to thank him for all the kind advice he gave me, and for the many invaluable comments on the text of this thesis.

Prohlášení

Prohlašuji, že jsem svou bakalářskou práci vypracoval samostatně a použil jsem pouze literaturu uvedenou v přiloženém seznamu.

Nemám závažný důvod proti užití tohoto školního díla ve smyslu § 60 Zákona č. 121/2000 Sb., o právu autorském, o právech souvisejících s právem autorským a o změně některých zákonů (autorský zákon).

V Praze dne 30. června 2011 ....

Štěpán Timr

Název práce: **Spektra hřebenových grafů**

Autor: Štěpán Timr

Obor: Matematické inženýrství

Druh práce: Bakalářská práce

Vedoucí práce: prof. RNDr. Pavel Exner, DrSc.

Abstrakt:
V této práci se zabýváme analýzou kvantových grafů ve tvaru nekonečného hřebene, tzn. sestávajících z přímky a nekonečného počtu úseček k ní připojených. Okrajové podmínky ve vrcholech grafu jsou přitom voleny tak, aby jimi definovaný laplacián příslušející grafu byl samosdružený. Provádíme analýzu pásového spektra v případě periodického systému a diskutujeme vliv lokálních poruch na spektrum.

Klíčová slova:
Kvantové grafy, laplacián, pásové spektrum, lokální poruchy

Title: **Spectra of Comb Graphs**

Author: Štěpán Timr

Abstract:
The work is devoted to analysis of quantum graphs in the form of an infinite comb, i.e. an infinite family of segments attached to a straight line through appropriate boundary conditions, defining Laplacian on such a graph as a self-adjoint operator. The band spectrum corresponding to the situation when such a system is periodic is analyzed. Furthermore, spectral consequences of local perturbations are discussed.

Key words:
Quantum graphs, Laplacian, band spectrum, local perturbations

Contents

Chapter 1

Introduction

Quantum graphs are simplified models developed to describe behavior of particles and waves in thin graph-like structures. Such structures are frequently encountered in nanotechnology and other disciplines dealing with mesoscopic systems. *Mesoscopic systems* are physical systems that are small enough to be described by means of quantum mechanics, and large enough to be designed and fabricated by today's experimentalists. As a typical example one can mention a network consisting of quantum wires, [1] in which quantum effects influence the motion of electrons. In order for those effects to appear, the transverse dimensions of such wires must be small enough (sometimes as small as a few atomic radii), and the purity of the material must be sufficiently high so that the mean free path of the electrons exceeds the lengths of the wires.

The approach taken by quantum graphs is to model such a quantum wire network as a metric graph equipped with a Hamiltonian (these terms will be specified in more detail in Chapter 2). Simply speaking, one replaces the wires with one-dimensional curves intersecting at point-like junctions (the former will represent the graph's edges, the latter its vertices) and solves the Schrödinger equation for a quantum particle living in such a system. At first place, one is usually interested in the spectrum of the quantum graph Hamiltonian, which is expected to exhibit a complex dependence on the topology and geometry of the graph, and on the choice of boundary conditions at the vertices.

In this work we address a particular example of an infinite periodic quantum graph possessing a comb-like geometry. The graph consists of a straight line to which an infinite number of equally long line segments is attached

[1] It remains to add that the range of applications of quantum graphs is by far not restricted to quantum wire networks. Quantum graphs are of interest in many other fields, such as waveguide theory, photonics or quantum chaos (see [Kuc02] for a detailed survey).

at uniform distances. We study the spectrum of a Hamiltonian defined as a negative second-derivative operator associated with the graph assuming a general class of local vertex conditions that guarantee its self-adjointness. It is shown that, except in a trivial case, the spectrum consists of an infinite number of spectral bands separated by open intervals, and implicit relations determining positions of spectral bands are derived both for positive and negative part of the spectrum. Apart from this, a necessary and sufficient condition for the existence of a negative spectral band is formulated, and a lower bound of the spectrum is given. Subsequently, we introduce a local perturbation by modifying the length of a selected "tooth" and/or the vertex conditions at the point of its attachment to the straight line. We derive implicit relations describing positions of newly arising eigenvalues in spectral gaps and then treat a simple tooth prolongation in more detail. Finally, we illustrate our findings with several examples of spectra calculated numerically for graphs exposed to local perturbations.

Chapter 2

General concepts

In this chapter we will introduce the general concept of the quantum graph as a metric graph equipped with a second-order differential operator. We will also discuss the family of vertex boundary conditions defining a self-adjoint extension of an operator.

2.1 Metric graphs

A *graph* is an ordered pair $\Gamma = (V,\, E)$ consisting of a set $V = \{v_i,\, i \in I\}$ of *vertices* and a set $E = \{e_j,\, j \in J\}$ of *edges* connecting the vertices. Each edge can be identified with a pair of vertices which represent the edge's endpoints. The pair can be either ordered or inordered. The former corresponds to an undirected graph, the latter to a directed one. The degree d_{v_i} of a vertex v_i expresses the number of edges containing v_i as one of its endpoints.

A graph Γ becomes a *metric graph* if each of its edges e_j is assigned a positive (finite or infinite) length l_j. Such a graph possesses a local metric in that each edge e_j is isometric with a finite or infinite real interval $[0,\, l_j]$. This enables us to introduce the Hilbert space of quadratically integrable functions defined on Γ as a direct sum of $L^2([0,\, l_j])$ for all edges e_j:

$$L^2(\Gamma) = \bigoplus_{j \in J} L^2([0,\, l_j]).$$

We will write the elements of $L^2(\Gamma)$ as $f = \{f_j\}$.

Let us add that in the case of an infinite graph, which will be of primary interest to us, one assumes that in any finite distance from each vertex, there is only a finite number of edges and other vertices. Such a graph is called *locally finite*.

2.2 Hamiltonians

Now that we have introduced the Hilbert space of quadratically integrable functions defined on Γ, we will mention a few typical examples of operators acting on that Hilbert space. Motivated by physical problems, one usually concentrates on second-order differential operators, for simplicity choosing the system of units in such a way that $\hbar/2m^* := 1$, where m^* is the effective mass of the electron. The most elementary case is a Hamiltonian acting as the negative Laplacian along each edge

$$f_j(x) \mapsto -\frac{d^2 f_j}{dx^2}(x) \tag{2.1}$$

for all $x \in (0,\, l_j)$. It corresponds to the free motion along the edges. Furthermore, one can include a scalar potential $V(x)$ as

$$f_j(x) \mapsto -\frac{d^2 f_j}{dx^2}(x) + V(x) f_j(x).$$

Another example is a general electromagnetic Hamiltonian defined as

$$f_j(x) \mapsto -\left(\frac{1}{i}\frac{d}{dx} - A(x)\right)^2 f_j(x) + V(x) f_j(x).$$

For the sake of simplicity, we will consider the first of these operators, given by the formula (2.1), in the following text and denote it by H.

For a complete definition of an operator, its domain must be specified. In the case of an operator defined on $L^2(\Gamma)$, the domain can be restricted by some boundary conditions imposed on the values of the functions f_j and their derivatives at the vertices. We will call these boundary conditions *vertex conditions*.

Typically, one requires the graph operator to be self-adjoint, which ensures that it can be interpreted as a quantum mechanical observable (see for example [BEH08] for details). We will determine the class of vertex conditions making the graph operator self-adjoint in the following section.

2.3 Vertex conditions

In this section, we will describe vertex conditions leading to a self-adjoint extension of the negative Laplacian H, acting according to (2.1). We will focus on vertex conditions being *local*, i.e. binding function and first-derivative values belonging to the corresponding vertex only. In order for the functions

f_j to have properly defined function and first-derivative values at the interval endpoints, we need to assume that $f_j \in H^2([0,\ l_j]) := H^2(e_j)$, the second-order Sobolev space, for all $j \in J$. The first-derivative values at the interval endpoints are then defined as

$$f'(0) = \lim_{x \to 0+} f'(x) = f'(0+), \quad f'(l_j) = -\lim_{x \to l_j -} f'(x) = -f'(l_j-),$$

i.e. always in the outgoing direction from the vertex.

Suppose that a vertex $v \in V$ has a degree d_v. Let F_v be the d_v-dimensional vector composed of function values at the edge endpoints incident to the vertex. At the same time, let F'_v stand for the d_v-dimensional vector comprising first-derivative values at those edge endpoints, taken in the outgoing directions from the vertex.

The vertex conditions at each vertex v can be written in a general form

$$A_v F_v + B_v F'_v = 0, \tag{2.2}$$

where A_v and B_v are square matrices of order d_v. Since we assume a second-order differential operator, we need two independent boundary conditions for each edge. Therefore, the number of independent conditions assigned to each vertex must be equal to its degree. Hence, we require the $d_v \times 2d_v$ matrix $(A_v,\ B_v)$ to have the maximal rank.

Let us assume that the domain $D(H)$ of the negative Laplacian H, acting according to (2.1), consists of functions $f \in L^2(\Gamma)$ such that

- $(\forall j \in J)(f_j \in H^2(e_j))$,
- $\sum_j \|f_j\|_{H^2(e_j)} < \infty$,
- f satisfies (2.2).

We will introduce a theorem which has its origin in [KS99] and gives a necessary and sufficient condition for the matrices A_v and B_v so that H is self-adjoint.

Theorem 2.3.1: *Let Γ be a metric graph and H be the negative Laplacian acting according to (2.1) with a domain $D(H)$ specified above. For each vertex $v \in V$ let the matrix $(A_v,\ B_v)$ have the maximal rank. Then H is self-adjoint if and only if the matrix*

$$A_v B_v^*$$

is self-adjoint for every vertex v.

As shown in [Kuc04], this theorem applies to both finite and countably infinite metric graphs, which is a consequence of the locality of vertex conditions.

Let v be a vertex of a degree d_v and $e_1, e_2 \dots, e_{d_v}$ the edges incident to this vertex. We will mention a few simple examples of vertex conditions with the self-adjointness property:

The δ-coupling One assumes that f is continuous at v, which implies that the functions $f_1, f_2 \dots, f_{d_v}$ attain the same value $f(v)$ at the interval endpoints incident to v. In addition, the first-derivative values at those interval endpoints, taken in the outgoing directions from v and denoted here by $f'_k(v)$, are bound by the following condition:

$$\sum_{k=1}^{d_v} f'_k(v) = \delta_v f(v),$$

where δ_v is a real parameter. In the case of $\delta_v = 0$, one gets the *free* or *Neumann (Kirchhoff)* condition. For the δ-coupling, the matrices A_v and B_v in (2.2) are given by

$$A_v = \begin{pmatrix} 1 & -1 & 0 & 0 & \cdots & 0 \\ 0 & 1 & -1 & 0 & \cdots & 0 \\ \vdots & \vdots & \vdots & \vdots & \ddots & \vdots \\ 0 & 0 & 0 & \cdots & 1 & -1 \\ -\delta_v & 0 & 0 & 0 & \cdots & 0 \end{pmatrix}, \quad B_v = \begin{pmatrix} 0 & 0 & \cdots & 0 \\ 0 & 0 & \cdots & 0 \\ 0 & 0 & \cdots & 0 \\ \vdots & \vdots & \ddots & \vdots \\ 1 & 1 & \cdots & 1 \end{pmatrix}.$$

The Dirichlet condition The simplest condition requires the values of $f_1, f_2 \dots, f_{d_v}$ at the interval endpoints incident to v to equal zero. This makes the edges effectively decoupled at v. It is evident that A_v now equals the identity matrix and B_v the zero matrix.

Let us add that the matrices A_v and B_v in the general expression (2.2) are not given uniquely. There are some other equivalent formulations of the condition (2.2), listed for example in [Kuc08] or [CET10].

In addition to the δ-coupling and the Dirichlet condition mentioned above, we will describe yet another example of vertex conditions in the following section.

2.4 Infinite comb

We will now introduce the unperturbed system studied in the rest of this work. As shown in Figure 2.1, the graph Γ consists of an infinite line on which vertices of type 1 are placed at uniform distances equal to a. To these vertices line segments of length c are attached. Their other ends form vertices of type 2. A function f from the Hilbert space $L^2(\Gamma)$ can be written as $f = \{f_p\}_{p=-\infty}^{+\infty} \cup \{g_p\}_{p=-\infty}^{+\infty}$.

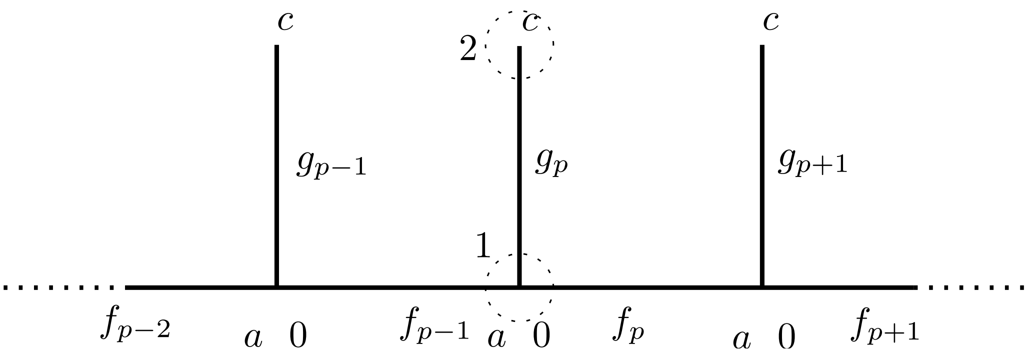

Figure 2.1: The unperturbed infinite comb Γ

The boundary conditions imposed on the type 1 vertices are

$$f_p(0) = f_{p-1}(a) \tag{2.3a}$$
$$g_p(0) = \beta f_{p-1}(a) + \gamma g_p'(0+) \tag{2.3b}$$
$$f_p'(0+) - f_{p-1}'(a-) = \delta f_{p-1}(a) - \beta g_p'(0+), \tag{2.3c}$$

where $p \in \mathbb{Z}$ and $\beta, \gamma, \delta \in \mathbb{R}$. The type 2 vertices are equipped with the Dirichlet condition

$$g_p(c) = 0. \tag{2.4}$$

A model consisting of a straight line equipped with one single finite-length appendix has already been studied in [EŠerešová94] assuming the same vertex conditions.

To verify that such vertex conditions guarantee the self-adjointness property, we will express them in the form (2.2). For the type 1 vertices we put

$$F_1 = \begin{pmatrix} f_{p-1}(a) \\ f_p(0) \\ g_p(0) \end{pmatrix}, \quad F_1' = \begin{pmatrix} f_{p-1}'(a) \\ f_p'(0) \\ g_p'(0) \end{pmatrix} = \begin{pmatrix} -f_{p-1}'(a-) \\ f_p'(0+) \\ g_p'(0+) \end{pmatrix}.$$

The matrices A_1 and B_1 are then

$$A_1 = \begin{pmatrix} 1 & -1 & 0 \\ -\beta & 0 & 1 \\ -\delta & 0 & 0 \end{pmatrix}, \quad B_1 = \begin{pmatrix} 0 & 0 & 0 \\ 0 & 0 & -\gamma \\ 1 & 1 & \beta \end{pmatrix}.$$

The matrix $A_1B_1^*$ becomes

$$A_1B_1^* = \begin{pmatrix} 0 & 0 & 0 \\ 0 & -\bar{\gamma} & -\beta + \bar{\beta} \\ 0 & 0 & -\delta \end{pmatrix} = \begin{pmatrix} 0 & 0 & 0 \\ 0 & -\gamma & 0 \\ 0 & 0 & -\delta \end{pmatrix}$$

since we assume that β, γ and δ are real. We see that $A_1B_1^*$ is self-adjoint if and only if $\beta, \gamma, \delta \in \mathbb{R}$. On this assumption, $A_1B_1^*$ satisfies the condition given by Theorem 2.3.1. The case of the type 2 vertices is trivial and therefore, we can conclude that the choice of the vertex conditions (2.3a)–(2.3c) and (2.4) guarantees the self-adjointness of the Hamiltonian H.

Finally, note that if $\beta = 0$, the teeth of the comb, i.e. the line segments of length c, become decoupled from the straight line. In this case, the system reduces to the Kronig-Penney model on the real line (studied in [AGHH04]) and an infinite number of independent subsystems created by the individual teeth. From now on we will assume $\beta \neq 0$ to exclude this simple case.

Chapter 3

Unperturbed system

In the following chapter we will examine the band spectrum of the Hamiltonian H acting according to (2.1) which is associated with the unperturbed comb Γ assuming the vertex conditions (2.3a)–(2.3c) and (2.4). We will treat the positive and negative part of the spectrum separately and finally derive a necessary and sufficient condition for the existence of a spectral band in the negative part of the spectrum.

3.1 Bloch-Floquet decomposition

The inspection of the continuous spectrum of H is significantly facilitated by the periodicity of Γ. It enables us to use the *Bloch-Floquet decomposition*, which makes it possible to work with one single unit cell instead of dealing with the whole infinite graph. However, before performing the Bloch-Floquet decomposition, we need to explain some theory behind it.

First, let us introduce the notion of a constant fiber direct integral. Suppose that $\mathcal{H}'$ is a separable Hilbert space and M is a space equipped with a σ-finite measure μ. Then we can construct the Hilbert space $L^2(M, d\mu, \mathcal{H}')$, consisting of square integrable $\mathcal{H}'$-valued functions defined on M. Such a Hilbert space is called a *constant fiber direct integral* and is written as

$$\mathcal{H} = \int_M^{\oplus} \mathcal{H}' \, d\mu.$$

Next, suppose that $A(.)$ is a function mapping M to the set of self-adjoint operators defined on $\mathcal{H}'$. We call $A(.)$ *measurable* if and only if the function $(A(.)+i)^{-1}$ is measurable. Given such a measurable operator-valued function, we can define an operator $A = \int_M^{\oplus} A(m)\, d\mu$ on the constant fiber direct integral $\mathcal{H}$ as

$$(A\psi)(m) = A(m)\psi(m)$$

for all $\psi \in D(A) \subset \mathcal{H}$ and for all $m \in M$. The domain $D(A)$ of the operator A contains functions $\psi \in \mathcal{H}$ satisfying

- $(\forall m \in M)(\psi(m) \in D(A(m)))$,
- $\int_M \|A(m)\psi(m)\|^2_{\mathcal{H}'} \, d\mu(m) < +\infty$.

An important thing for us is the relation between the spectra $\sigma(A(m))$ of the fibers $A(m)$ and the spectrum $\sigma(A)$ of A, described in the following theorem (see Theorem XIII.85 in [RS78]):

Theorem 3.1.1: *Let $A = \int_M^{\oplus} A(m) \, d\mu$ where $A(.)$ is measurable and $A(m)$ is self-adjoint for each $m \in M$. Then:*

1. *The operator A is self-adjoint.*
2. *$\lambda \in \sigma(A)$ if and only if for all $\epsilon > 0$ the set of $m \in M$ such that $\sigma(A(m)) \cap (\lambda - \epsilon, \lambda + \epsilon) \neq \emptyset$ has a nonzero measure.*
3. *λ is an eigenvalue of A if and only if the set of $m \in M$ such that λ is an eigenvalue of $A(m)$ has a nonzero measure.*

In the particular case of the infinite comb Γ, the space $L^2(\Gamma)$ can be decomposed as

$$L^2(\Gamma) = U^{-1} L^2([-\pi, \pi), d\theta, L^2(\Gamma_0)) = U^{-1} \int_{[-\pi, \pi)}^{\oplus} L^2(\Gamma_0) \, d\theta$$

in analogy with the decomposition of $L^2(\mathbb{R})$ described in [RS78], Section XIII.16. The Brillouin zone $[-\pi, \pi)$ plays the role of the measure space M and the fiber $\mathcal{H}'$ is formed by $L^2(\Gamma_0) = L^2([-a/2, 0]) \oplus L^2([0, a/2]) \oplus L^2([0, c])$. The unit cell Γ_0 is depicted in Figure 3.1. For every $\varphi \in \int_{[-\pi, \pi)}^{\oplus} L^2(\Gamma_0) \, d\theta$ and every $\theta \in [-\pi, \pi)$ let the function $\varphi(\theta, .) = \{\varphi_L(\theta, .), \varphi_R(\theta, .), \varphi_T(\theta, .)\}$ be the corresponding element of $L^2(\Gamma_0)$. U is then a unitary operator

$$U : \quad f \in L^2(\Gamma) \mapsto \varphi \in \int_{[-\pi, \pi)}^{\oplus} L^2(\Gamma_0) \, d\theta$$

with φ given by

$$\varphi_L(\theta, x) = \sum_{p=-\infty}^{+\infty} e^{ip\theta} f_{p-1}(x + a), \quad x \in [-a/2, 0], \, \theta \in [-\pi, \pi), \tag{3.1}$$

$$\varphi_R(\theta, x) = \sum_{p=-\infty}^{+\infty} e^{ip\theta} f_p(x), \quad x \in [0, a/2], \, \theta \in [-\pi, \pi), \tag{3.2}$$

$$\varphi_T(\theta, x) = \sum_{p=-\infty}^{+\infty} e^{ip\theta} g_p(x), \quad x \in [0, c], \, \theta \in [-\pi, \pi). \tag{3.3}$$

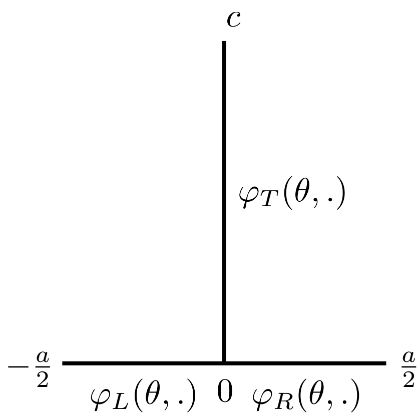

Figure 3.1: The unit cell Γ_0

The negative Laplacian H defined on $L^2(\Gamma)$ can then be decomposed as

$$UHU^{-1} = \int_{[0,\,2\pi)}^{\oplus} H(\theta)\,\frac{d\theta}{2\pi},$$

where $H(\theta)$ is the negative Laplacian defined on $L^2(\Gamma_0)$ with the domain $D(H(\theta))$ comprising functions $\varphi(\theta, .) = \{\varphi_L(\theta, .),\, \varphi_R(\theta, .),\, \varphi_T(\theta, .)\}$ which satisfy boundary conditions of type (2.3a)–(2.3c) and (2.4), i.e.

$$\varphi_R(\theta, 0) = \varphi_L(\theta, 0) \tag{3.4a}$$

$$\varphi_T(\theta, 0) = \beta\varphi_L(\theta, 0) + \gamma\varphi_T'(\theta, 0+) \tag{3.4b}$$

$$\varphi_R'(\theta, 0+) - \varphi_L'(\theta, 0-) = \delta\varphi_L(\theta, 0) - \beta\varphi_T'(\theta, 0+) \tag{3.4c}$$

and

$$\varphi_T(\theta, c) = 0. \tag{3.5}$$

In addition, there are two more boundary conditions imposed on the endpoints of the unit cell:

$$\varphi_R(\theta, a/2) = e^{i\theta}\varphi_L(\theta, -a/2) \tag{3.6a}$$

$$\varphi_R'(\theta, a/2) = e^{i\theta}\varphi_L'(\theta, -a/2). \tag{3.6b}$$

Equipped with the apparatus of the Bloch-Floquet decomposition introduced above, we can examine $\sigma(H)$ by looking at the spectra of $H(\theta)$. For every $\theta \in [-\pi,\, \pi)$ the operator $H(\theta)$ has a compact resolvent and therefore, its spectrum is purely discrete. As a result, $k^2 \in \mathbb{R}$ belongs to $\sigma(H(\theta))$ if and only if there exists an eigenfunction $\varphi(\theta, .) = \{\varphi_L(\theta, .),\, \varphi_R(\theta, .),\, \varphi_T(\theta, .)\} \in D(H(\theta)) \subset L^2(\Gamma_0)$ corresponding to k^2.

Based on a general result in [EKW10] applied to our graph, we are able to predict that the edges of the spectral bands potentially present in $\sigma(H)$ are attained at $\theta = 0$ or $\theta = -\pi$.

3.2 Positive part of the spectrum

Let us suppose that $k > 0$. The eigenfunction candidate is expected to have the following form:

$$\varphi_L(\theta, x) = r(k)\cos kx + s(k)\sin kx, \quad x \in [-a/2,\, 0], \tag{3.7a}$$
$$\varphi_R(\theta, x) = t(k)\cos kx + u(k)\sin kx, \quad x \in [0,\, a/2], \tag{3.7b}$$
$$\varphi_T(\theta, x) = v(k)\cos kx + w(k)\sin kx, \quad x \in [0,\, c], \tag{3.7c}$$

where $r(k)$, $s(k)$, $t(k)$, $u(k)$, $v(k)$ and $w(k)$ are complex coefficients depending on k. The use of this Ansatz enables us to formulate the following statement:

Proposition 3.2.1: *Let $\theta \in [-\pi, \pi)$, $k > 0$, $k \notin \left\{\frac{m\pi}{a} | m \in \mathbb{N}\right\}$ and $\sin kc + \gamma k \cos kc \neq 0$. Then $k^2 \in \sigma(H(\theta))$ if and only if the following condition is satisfied:*

$$\cos\theta = \cos ka + \frac{\sin ka}{2} A(k) := B(k), \tag{3.8}$$

where

$$A(k) = \left(\frac{\delta}{k} + \frac{\beta^2 \cos kc}{\sin kc + k\gamma \cos kc}\right).$$

Proof. By substituting the Ansatz (3.7a)–(3.7c) into the conditions (3.4a)–(3.4c), (3.5), (3.6a) and (3.6b), we get the following set of equations for the coefficients $r(k)$, $s(k)$, $t(k)$, $u(k)$, $v(k)$ and $w(k)$:

$$r(k) = t(k) \tag{3.9a}$$
$$v(k) = \beta r(k) + \gamma w(k) k \tag{3.9b}$$
$$u(k)k - s(k)k = \delta r(k) - \beta w(k) k \tag{3.9c}$$
$$v(k)\cos kc + w(k)\sin kc = 0 \tag{3.9d}$$
$$t(k)\cos\frac{ka}{2} + u(k)\sin\frac{ka}{2} = e^{i\theta}(r(k)\cos\frac{ka}{2} - s(k)\sin\frac{ka}{2}) \tag{3.9e}$$
$$-t(k)\sin\frac{ka}{2} + u(k)\cos\frac{ka}{2} = e^{i\theta}(r(k)\sin\frac{ka}{2} + s(k)\cos\frac{ka}{2}). \tag{3.9f}$$

By using the first four equations, we are able to express the coefficients $t(k)$, $u(k)$, $v(k)$ and $w(k)$ as multiples of $r(k)$ and $s(k)$. Subsequently, from the fifth and the sixth equation it follows that

$$\left(\cos\frac{ka}{2}\left(1 - e^{i\theta}\right) + \sin\frac{ka}{2} A(k)\right) r(k) = -\sin\frac{ka}{2}\left(1 + e^{i\theta}\right) s(k) \tag{3.10a}$$
$$\left(\sin\frac{ka}{2}\left(1 + e^{i\theta}\right) - \cos\frac{ka}{2} A(k)\right) r(k) = \cos\frac{ka}{2}\left(1 - e^{i\theta}\right) s(k) \tag{3.10b}$$

If $\theta \in (-\pi, 0) \cup (0, \pi)$, by expressing $s(k)$ from both (3.10a) and (3.10b), and comparing these two expressions, we obtain the relation (3.8), which forms a necessary and sufficient condition for the existence of a nontrivial solution of (3.9a)–(3.9f). In the case of $\theta = -\pi$ we get from (3.10a) that

$$2\cos\frac{ka}{2} + \sin\frac{ka}{2}A(k) = 0 \tag{3.11}$$

since $r(k)$ must not be equal to zero: if $r(k)$ was equal to zero, it would follow from (3.10b) that $s(k)$ also equals zero and the resulting function would be the zero function. The condition (3.11) can be rewritten as

$$-1 = \cos ka + \frac{\sin ka}{2}A(k)$$

which is merely a special case of (3.8) given $\theta = -\pi$. The case of $\theta = 0$ can be treated analogously. □

Let us now look at the special cases of $k \in \left\{\frac{m\pi}{a} | m \in \mathbb{N}\right\}$ and $\sin kc + k\gamma\cos kc = 0$, which we did not include in the previous proposition.

Proposition 3.2.2: *Let* $k \in \left\{\frac{m\pi}{a} | m \in \mathbb{N}\right\}$ *and* $\sin kc + k\gamma\cos kc \neq 0$.

- *If* $m = 2l$, $l \in \mathbb{N}$, *then* $k^2 \in \sigma(H(0))$ *and* $k^2 \notin \sigma(H(\theta))$ *for* $\theta \neq 0$.
- *If* $m = 2l - 1$, $l \in \mathbb{N}$, *then* $k^2 \in \sigma(H(-\pi))$ *and* $k^2 \notin \sigma(H(\theta))$ *for* $\theta \neq -\pi$.

Proof. Let $m = 2l$, $l \in \mathbb{N}$. Again, we want the set of equations (3.9a)–(3.9f) for the eigenfunction coefficients to have a nontrivial solution. Like in the proof of the previous proposition, we can express the coefficients $t(k)$, $u(k)$, $v(k)$ and $w(k)$ as multiples of $r(k)$ and $s(k)$. The equations (3.10a) and (3.10b) turn into

$$\left(1 - e^{i\theta}\right) r(k) = 0$$

and

$$A(k)r(k) = -\left(1 - e^{i\theta}\right) s(k),$$

from which it is evident that there exists a nonzero solution of (3.9a)–(3.9f) if and only if $\theta = 0$.

For $m = 2l - 1$, $l \in \mathbb{N}$, the equations (3.10a) and (3.10b) transform into

$$A(k)r(k) = -\left(1 + e^{i\theta}\right) s(k)$$

and

$$\left(1 + e^{i\theta}\right) r(k) = 0$$

with a nontrivial solution if and only if $\theta = -\pi$.

□

For a positive k satisfying $\sin kc + k\gamma \cos kc = 0$ we will see that k^2 belongs to $\sigma(H)$ if and only if $k \in \left\{\frac{m\pi}{a} | m \in \mathbb{N}\right\}$, and, based on Theorem 3.1.1, that such a k^2 is an eigenvalue of H. Furthermore, we will find out that this eigenvalue necessarily becomes an isolated point of $\sigma(H)$:

Proposition 3.2.3: *Let $k > 0$ satisfy $\sin kc + k\gamma \cos kc = 0$. Then:*

- *For all $\theta \in [-\pi, \pi)$ it holds that $k^2 \in \sigma(H(\theta))$ if and only if $k \in \left\{\frac{m\pi}{a} | m \in \mathbb{N}\right\}$.*
- *There exists an $\epsilon > 0$ such that $\sigma(H(\theta)) \cap (k^2 - \epsilon,\, k^2 + \epsilon) \backslash \{k^2\} = \emptyset$ for all $\theta \in [-\pi, \pi)$.*

Proof. If $\sin kc + k\gamma \cos kc = 0$ and $k \in \left\{\frac{m\pi}{a} | m \in \mathbb{N}\right\}$, it can be shown that the function $\varphi(\theta, .) = \{\varphi_L(\theta, .),\, \varphi_R(\theta, .),\, \varphi_T(\theta, .)\}$ defined either as

$$\begin{aligned}
\varphi_L(\theta,\, x) &= \left(e^{i\theta} - 1\right) \sin k(x + a), \quad x \in [-a/2,\, 0], \\
\varphi_R(\theta,\, x) &= \left(1 - e^{-i\theta}\right) \sin kx, \quad x \in [0,\, a/2], \\
\varphi_T(\theta, x) &= \left(e^{i\theta} - e^{-i\theta}\right) \frac{\cos ka}{\beta} \left(\sin kx - \tan kc \cos kx\right), \quad x \in [0,\, c].
\end{aligned}$$

or as

$$\begin{aligned}
\varphi_L(\theta,\, x) &= \left(e^{i\theta} + 1\right) \sin k(x + a), \quad x \in [-a/2,\, 0], \\
\varphi_R(\theta,\, x) &= \left(1 + e^{-i\theta}\right) \sin kx, \quad x \in [0,\, a/2], \\
\varphi_T(\theta, x) &= \frac{\tan kc}{\beta} \left(2 - \left(e^{i\theta} + e^{-i\theta}\right) \cos ka\right) \cos kx \\
&\quad + \frac{1}{\beta} \left(\left(e^{i\theta} + e^{-i\theta}\right) \cos ka - 2\right) \sin kx, \quad x \in [0,\, c].
\end{aligned}$$

satisfies the conditions (3.4a)–(3.4c), (3.5), (3.6a) and (3.6b). The choice of these functions may now seem like a random guess, but it will be justified later in Chapter 4. On the other hand, given a $k > 0$ such that $\sin kc + k\gamma \cos kc = 0$ and $k \notin \left\{\frac{m\pi}{a} | m \in \mathbb{N}\right\}$, from the equations (3.9a)–(3.9f) we obtain that $r(k) = s(k) = t(k) = u(k) = v(k) = w(k) = 0$, which corresponds to the zero function.

To prove the second part of the proposition, we will compute $\lim_{x \to k} B(x)$ with $B(.)$ originating from the spectral condition (3.8) and k satisfying $\sin kc + k\gamma \cos kc = 0$. Suppose first that $k \in \left\{\frac{m\pi}{a} | m \in \mathbb{N}\right\}$, too. Given $(c + \gamma) - k\gamma c \tan kc \neq 0$, we get from l'Hôpital's rule that

$$\lim_{x \to k} B(x) = \frac{(-1)^m a/2}{(c + \gamma) - k\gamma c \tan kc}.$$

If $(c+\gamma)-k\gamma c\tan kc = 0$, the limit equals simply $(-1)^m \cdot (+\infty)$. We will show that $|\lim_{x\to k} B(x)| > 1$ even in the former case: Suppose that $|\lim_{x\to k} B(x)| \leq 1$. This can be rewritten as

$$-2 \leq \frac{a/2}{(c+\gamma) - k\gamma c\tan kc} \leq 0$$

or equivalently as

$$(c+\gamma) - k\gamma c\tan kc \leq -\frac{a}{4}$$

Since γ can be expressed as $\gamma = -\frac{\tan kc}{k}$ and a as $a = \frac{m\pi}{k}$, we reformulate the condition as

$$c - \frac{\tan kc}{k} + c\tan^2 kc \leq -\frac{m\pi}{4k},$$

which after multiplying by k and substituting $z = kc$ transforms into

$$z(\tan^2 z + 1) - \tan z + \frac{m\pi}{4} \leq 0.$$

It is not difficult to show that the expression $z(\tan^2 z+1)-\tan z+\frac{m\pi}{4}$ remains positive for all $z > 0$: For $z \in (0,\, 1)$ it can be estimated from below as

$$z(\tan^2 z + 1) - \tan z + \frac{m\pi}{4} > z - \tan z + \frac{m\pi}{4} > 0$$

since $\tan z - z < \tan 1 - 1 < \frac{m\pi}{4}$ on $(0,\, 1)$. On the other hand, if $z \in [1,\, +\infty)$, it holds that

$$z(\tan^2 z + 1) - \tan z + \frac{m\pi}{4} > \tan^2 z - \tan z + \frac{m\pi}{4} > 0.$$

This contradicts the assumption $|\lim_{x\to k} B(x)| \leq 1$. Finally, if $k \notin \left\{\frac{m\pi}{a} | m \in \mathbb{N}\right\}$, it is evident that $|\lim_{x\to k} B(x)| = +\infty$. Therefore, we can conclude that there exists a neighborhood of k^2 that does not contain any element of $\sigma(H(\theta))$ for any $\theta \in [-\pi,\, \pi)$. $\square$

Let us add that the eigenvalue observed in the case of a $k \in \left\{\frac{m\pi}{a} | m \in \mathbb{N}\right\}$ satisfying $\sin kc + k\gamma\cos kc = 0$ actually corresponds to a degenerated spectral band of H, that is, the eigenvalue has an infinite multiplicity; from our results in Chapter 4 it will be evident that there is an infinite number of mutually orthogonal eigenfunctions with compact supports corresponding to it.

In order to uncover the character of the positive spectral bands and edges present in $\sigma(H)$, let us rewrite the condition determining the positive part of the continuous spectrum of H

$$|B(k)| = \left|\cos ka + \frac{\sin ka}{2} A(k)\right| \leq 1,$$

following from Proposition 3.2.1, in a different way as

$$2\tan\frac{ka}{2} \leq A(k) \leq 2\tan\frac{ka+\pi}{2} \tag{3.12}$$

for $k \in \left(\frac{(2l-1)\pi}{a}, \frac{2l\pi}{a}\right)$, $l \in \mathbb{N}$, and

$$2\tan\frac{ka}{2} \geq A(k) \geq 2\tan\frac{ka+\pi}{2} \tag{3.13}$$

for $k \in \left(\frac{2l\pi}{a}, \frac{(2l+1)\pi}{a}\right)$, $l \in \mathbb{N}$. The conditions (3.12) and (3.13) can be visualized as shown in Figure 3.2. It is easy to realize that for any choice of the lengths a and c, and parameters β, γ and δ (keeping in mind the assumption $\beta \neq 0$, mentioned above) the positive part of $\sigma(H)$ contains an infinite number of spectral bands.

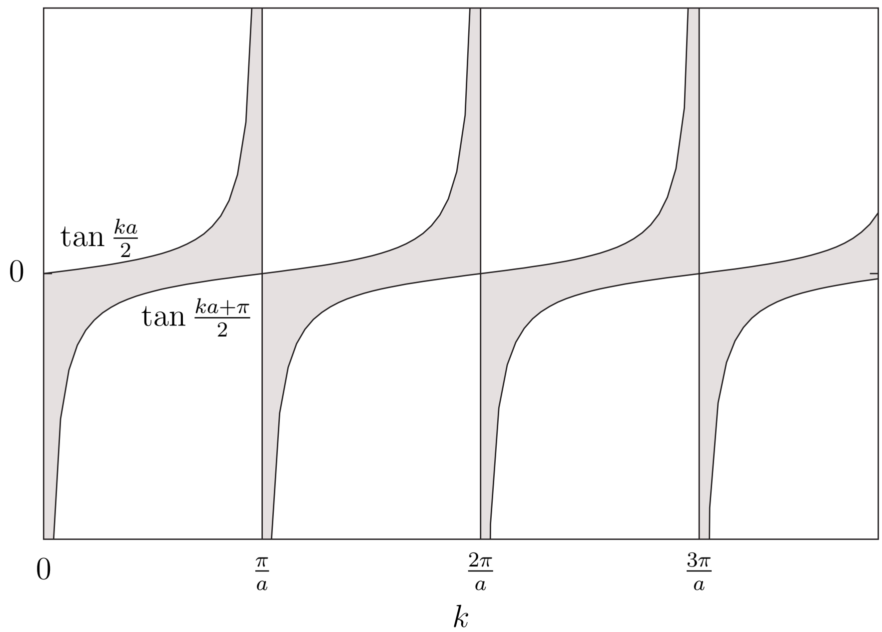

Figure 3.2: Permissible values of $A(k)$ for k^2 to belong to the continuous part of $\sigma(H)$

Furthermore, if we assume a choice of parameters β, γ and δ such that $A(.)$ decreases monotonically on $(0, +\infty)$ except at its points of discontinuity, we can divide the gaps between the spectral bands into the following two groups:

1. exactly one of the gap edges belongs to $\left\{\frac{m^2\pi^2}{a^2} | m \in \mathbb{N}_0\right\}$,

2. neither of the gap edges belongs to $\left\{\frac{m^2\pi^2}{a^2}|m \in \mathbb{N}_0\right\}$ and there is a point k^2 within the spectral gap satisfying $\sin kc + k\gamma \cos kc = 0$.

A point k^2 such that $\sin kc + k\gamma \cos kc = 0$, located within a spectral gap, turns into an eigenvalue if k happens to be an element of $\left\{\frac{m\pi}{a}|m \in \mathbb{N}\right\}$ at the same time.

Finally, let us add that every point $k^2 \in \left\{\frac{m^2\pi^2}{a^2}|m \in \mathbb{N}\right\}$ is located on the edge of a spectral band unless $A(.)$ attains zero at k. In the latter case, such a k^2 may be found within a spectral band.

3.3 Zero and negative part of the spectrum

To answer the question of when $0 \in \sigma(H(\theta))$, one can use an Ansatz in the form

$$\varphi_L(\theta, x) = r(k) + s(k)x, \quad x \in [-a/2, 0], \tag{3.14a}$$

$$\varphi_R(\theta, x) = t(k) + u(k)x, \quad x \in [0, a/2], \tag{3.14b}$$

$$\varphi_T(\theta, x) = v(k) + w(k)x, \quad x \in [0, c]. \tag{3.14c}$$

It is then possible to formulate the following statement:

Proposition 3.3.1: $0 \in \sigma(H(\theta))$ *if and only if* $c \neq -\gamma$ *and*

$$\cos\theta = 1 + \frac{a}{2}\left(\delta + \frac{\beta^2}{c+\gamma}\right).$$

Proof. This statement can be verified in analogy with Proposition 3.2.1 by substituting the Ansatz (3.14a)–(3.14c) into the conditions (3.4a)–(3.4c), (3.5), (3.6a) and (3.6b). □

The negative parts of $\sigma(H(\theta))$ can be examined by replacing k with $i\kappa$, $\kappa > 0$, in the considerations dealing with the positive parts. The result is the following:

Proposition 3.3.2: *Let* $\theta \in [-\pi, \pi)$, $\kappa > 0$ *and* $\sinh \kappa c + \kappa\gamma \cosh \kappa c \neq 0$. *Then* $-\kappa^2 \in \sigma(H(\theta))$ *if and only if the following condition is satisfied:*

$$\cos\theta = \cosh \kappa a + \frac{\sinh \kappa a}{2}\tilde{A}(\kappa) := \tilde{B}(\kappa), \tag{3.15}$$

where

$$\tilde{A}(\kappa) = \left(\frac{\delta}{\kappa} + \frac{\beta^2 \cosh \kappa c}{\sinh \kappa c + \kappa\gamma \cosh \kappa c}\right).$$

However, if a $\kappa > 0$ *satisfies* $\sinh \kappa c + \kappa\gamma \cosh \kappa c = 0$, *then* $-\kappa^2 \notin \sigma(H(\theta))$ *for all* $\theta \in [-\pi, \pi)$.

3.3.1 Existence of negative spectral bands

In this subsection we will attempt to derive a necessary and sufficient condition for the negative part of the continuous spectrum of H to be nonempty.

Based on Proposition 3.3.2, we know that $-\kappa^2$, $\kappa > 0$, belongs to the continuous part of $\sigma(H)$ if and only if

$$\left|\tilde{B}(\kappa)\right| \leq 1.$$

In analogy with the positive case, this condition can be reformulated as

$$-2\coth\frac{\kappa a}{2} \leq \tilde{A}(\kappa) \leq -2\tanh\frac{\kappa a}{2}, \tag{3.16}$$

which is to be solved graphically. In other words, we need to look for combinations of parameters a, c, β, γ and δ such that $\tilde{A}(.)$ intersects the area depicted in Figure 3.3.

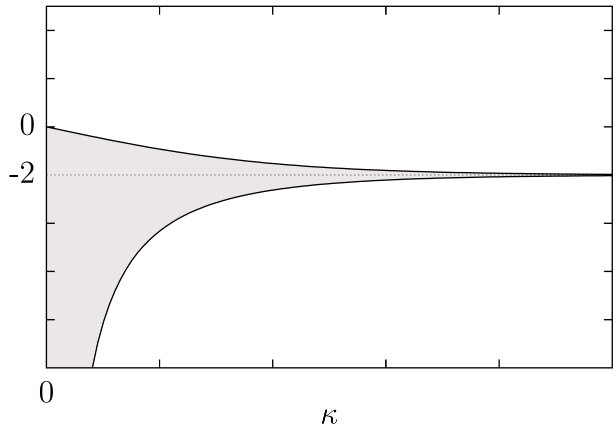

Figure 3.3: Permissible values of $\tilde{A}(\kappa)$ for $-\kappa^2$ to belong to the continuous part of the spectrum

The first thing one should realize is that $\lim_{\kappa\to\infty}\tilde{A}(\kappa)$ equals zero for $\gamma \neq 0$ and β^2 for $\gamma = 0$. Therefore, a sufficient condition for the existence of a negative spectral band is $\lim_{\kappa\to 0+}\tilde{A}(\kappa)$ being lower than zero.

Lemma 3.3.1: $\lim_{\kappa\to 0+}\tilde{A}(\kappa)$ *equals to*

- $-\infty$ *for* $\delta + \frac{\beta^2}{c+\gamma} < 0$ *or* $\gamma = -c$,
- *0 for* $\delta + \frac{\beta^2}{c+\gamma} = 0$,

- $+\infty$ *for* $\delta + \frac{\beta^2}{c+\gamma} > 0$.

Proof. After some manipulations and by applying l'Hôpital's rule, we get that

$$\lim_{\kappa\to 0+} \tilde{A}(\kappa) = \lim_{\kappa\to 0+} \left(\frac{\delta(c+\gamma)+\beta^2}{\kappa(c+2\gamma)+\tanh\kappa c(1+\gamma c\kappa^2)} + \kappa \cdot R(\kappa) \right), \tag{3.17}$$

where $R(.)$ is a function bounded by a constant on a right neighborhood of zero. Let us put

$$D(\kappa) := \kappa(c+2\gamma) + \tanh\kappa c(1+\gamma c\kappa^2).$$

We get $D(0) = 0$ and $D'(0) = c+\gamma$. Hence, if $\gamma \neq -c$, there exists an $\epsilon > 0$ such that $\operatorname{sgn} D(\kappa) = \operatorname{sgn}(c+\gamma)$ for all $\kappa \in (0, \epsilon)$. In combination with (3.17), we obtain

$$\lim_{\kappa\to 0+} \tilde{A}(\kappa) = \operatorname{sgn}(\delta(c+\gamma)+\beta^2) \cdot \operatorname{sgn}(c+\gamma) \cdot (+\infty) = \operatorname{sgn}(\delta + \frac{\beta^2}{c+\gamma}) \cdot (+\infty).$$

for $\gamma \neq -c$, $\delta + \frac{\beta^2}{c+\gamma} \neq 0$, and

$$\lim_{\kappa\to 0+} \tilde{A}(\kappa) = 0$$

for $\gamma \neq -c$, $\delta + \frac{\beta^2}{c+\gamma} = 0$. Finally, let us examine the case $\gamma = -c$. By substituting $\gamma = -c$ into (3.17) we get that

$$\lim_{\kappa\to 0+} \tilde{A}(\kappa) = \lim_{\kappa\to 0+} \left(\frac{\beta^2}{\tanh\kappa c(1-\kappa^2 c^2) - \kappa c} + \kappa \cdot R(\kappa) \right).$$

We will prove that the denominator, expressed as $\tanh x \cdot (1-x^2) - x$, $x = \kappa c$, is negative on a right neighborhood of zero: Provided $0 < x = \kappa c < 1$, the inequality $\tanh x \cdot (1-x^2) - x < 0$ can be rewritten equivalently as

$$\tanh x - \frac{x}{1-x^2} < 0.$$

By performing a third-order Taylor expansion of $\tanh x$ and $\frac{x}{1-x^2}$ at zero, we obtain

$$\tanh x - \frac{x}{1-x^2} = -\frac{4}{3}x^3 + O(x^4),$$

which ensures that $\tanh x - \frac{x}{1-x^2}$ is really negative on a right neighborhood of zero. Based on this, we conclude that $\lim_{\kappa\to 0+} \tilde{A}(\kappa) = -\infty$ for $\gamma = -c$. □

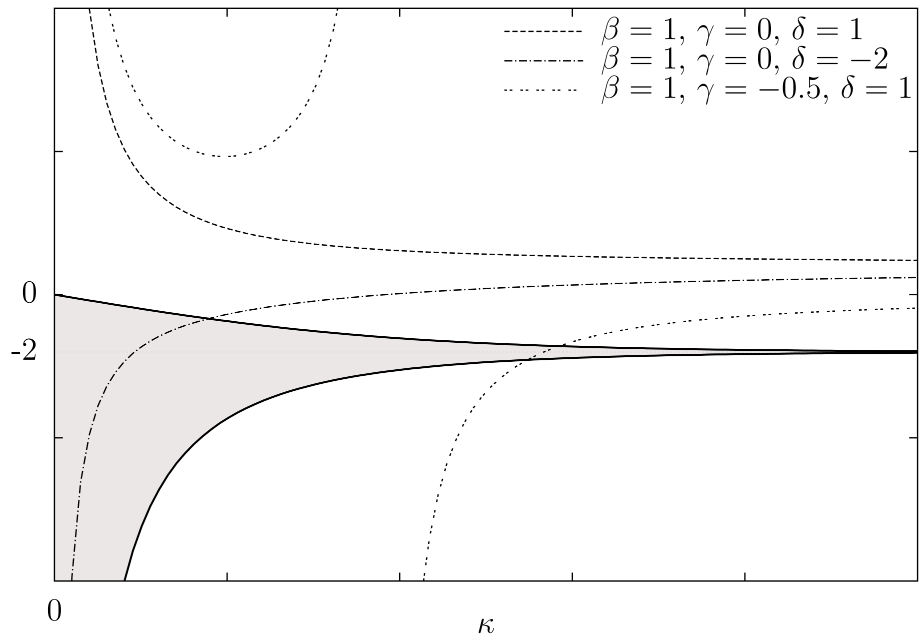

Figure 3.4: Shapes of $\tilde{A}(.)$ for different parameter values; $a = 1$, $c = 1$

From the statement just proven, we see that if $\delta + \frac{\beta^2}{c+\gamma} < 0$ or $\gamma = -c$, the existence of a negative spectral band is guaranteed. Apart from that, let us mention that $\tilde{A}(.)$ is continuous on $(0, +\infty)$ except at points satisfying $\sinh \kappa c + \kappa\gamma \cosh \kappa c = 0$. As we shall see, the presence of such a discontinuity guarantees the existence of a negative spectral band, as well.

First, let us examine the presence of a point satisfying $\sinh \kappa c + \kappa\gamma \cosh \kappa c = 0$ in $(0, +\infty)$ depending on γ. The equation can be rewritten as

$$\tanh \kappa c = -\kappa\gamma. \tag{3.18}$$

As demonstrated in Figure 3.5, it follows from the properties of tanh that the equation (3.18) has exactly one solution on $(0, +\infty)$ if and only if $\gamma \in (-c, 0)$ and no solutions in the remaining cases. In addition, denoting the point that satisfies the equation (3.18) by κ_0, we get for all $\kappa \in (\kappa_0, +\infty)$ that $\tanh \kappa c < -\kappa\gamma$, or $\tanh \kappa c + \kappa\gamma < 0$ and therefore, $\lim_{\kappa \to \kappa_0+} \tilde{A}(\kappa) = -\infty$, which ensures the existence of a spectral band in $(-\infty, -\kappa^2)$. Thus, based on this and the previous statements, we can conclude that if $\gamma \in [-c, 0)$ or $\delta + \frac{\beta^2}{c+\gamma} < 0$, there exists a negative spectral band in the spectrum of H.

In the remaining case, namely $\gamma \notin [-c, 0)$ and $\delta + \frac{\beta^2}{c+\gamma} \geq 0$, we will prove that $\tilde{A}(\kappa)$ stays positive for all $\kappa \in (0, +\infty)$, which excludes the existence of a

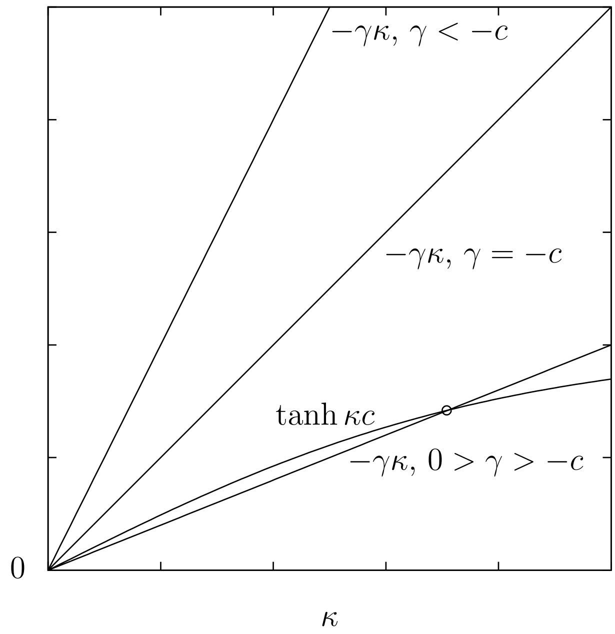

Figure 3.5

negative spectral band (see the condition (3.16)). First, let us take $\gamma \notin [-c,\, 0)$ and $\delta + \frac{\beta^2}{c+\gamma} = 0$. We get

$$\tilde{A}(\kappa) = -\frac{\beta^2}{\kappa(c+\gamma)} + \frac{\beta^2 \cosh \kappa c}{\sinh \kappa c + \kappa\gamma \cosh \kappa c} = \frac{\beta^2(\kappa c - \tanh \kappa c)}{(\kappa c + \kappa\gamma)(\tanh \kappa c + \kappa\gamma)}. \tag{3.19}$$

We can make use of the fact that $\tanh x < x$ for all $x \in (0,\, +\infty)$. Hence, the numerator in (3.19) is always positive. Furthermore, the signs of $\kappa c + \kappa\gamma$ and $\tanh \kappa c + \kappa\gamma$ remain the same, which causes the denominator to stay positive, as well. Therefore, we get that $\tilde{A}(\kappa) > 0$ for all $\kappa \in (0,\, +\infty)$. For $\gamma \notin [-c,\, 0)$ and $\delta + \frac{\beta^2}{c+\gamma} > 0$ we finally obtain

$$\tilde{A}(\kappa) = \frac{\delta}{\kappa} + \frac{\beta^2 \cosh \kappa c}{\sinh \kappa c + \kappa\gamma \cosh \kappa c} > -\frac{\beta^2}{\kappa(c+\gamma)} + \frac{\beta^2 \cosh \kappa c}{\sinh \kappa c + \kappa\gamma \cosh \kappa c} > 0,$$

given $\kappa \in (0,\, +\infty)$.

Now we are ready to formulate the necessary and sufficient condition for the existence of a negative spectral band:

Proposition 3.3.3: *The continuous spectrum of H has a nonempty negative part if and only if* $\gamma \in [-c,\, 0) \vee \delta + \frac{\beta^2}{c+\gamma} < 0$.

3.3.2 Lower bound of the continuous spectrum

When trying to localize positions of spectral bands numerically, it proves useful to have at least a rough estimate of the position of the lowest spectral band. If the negative part of the continuous spectrum of H is empty, zero can well serve as its lower bound. However, provided the negative part of the continuous spectrum of H is nonempty, i.e. $\gamma \in [-c, 0) \vee \delta + \frac{\beta^2}{c+\gamma} < 0$, a lower bound is given by the following proposition.

Proposition 3.3.4: *The continuous spectrum of H has a lower bound equal to $-b^2$, where b is given as*

$$b = \max\left(\frac{1}{a}, \frac{2}{|\gamma|}, \frac{\frac{|\delta|}{2} + \frac{\beta^2}{|\gamma|}}{\tanh(1/2)}\right)$$

if $\gamma \neq 0$, and

$$b = \frac{|\delta|}{\beta^2}$$

if $\gamma = 0$.

Proof. Suppose first that $\gamma = 0$. It is easy to see that if $\kappa > \frac{|\delta|}{\beta^2}$, then $\tilde{A}(\kappa)$ is greater than zero and therefore, the condition (3.16) cannot be satisfied.

If $\gamma \neq 0$, we will find a $b \in (0, +\infty)$ such that $\tilde{A}(\kappa) > -2\tanh\frac{\kappa a}{2}$ for all $\kappa > b$. Let us suppose that $\kappa > \frac{1}{a}$. Then $-2\tanh\frac{\kappa a}{2} < -2\tanh\frac{1}{2}$. As a next step, we will derive an upper estimate of $\left|\tilde{A}(\kappa)\right|$ given $\kappa > \frac{2}{|\gamma|}$. We obtain

$$\left|\tilde{A}(\kappa)\right| = \left|\frac{\delta}{\kappa} + \frac{\beta^2}{\tanh\kappa c + \kappa\gamma}\right| \leq \frac{|\delta|}{\kappa} + \frac{\beta^2}{\kappa\,|\gamma| - 1} < \frac{|\delta| + \frac{2\beta^2}{|\gamma|}}{\kappa}.$$

Now, putting $b = \max\left(\frac{1}{a}, \frac{2}{|\gamma|}, \frac{\frac{|\delta|}{2} + \frac{\beta^2}{|\gamma|}}{\tanh(1/2)}\right)$, we get for all $\kappa > b$ that

$$\left|\tilde{A}(\kappa)\right| < \frac{|\delta| + \frac{2\beta^2}{|\gamma|}}{\kappa} \leq 2\tanh\frac{1}{2} < 2\tanh\frac{\kappa a}{2}$$

and therefore, $\tilde{A}(\kappa) > -2\tanh\frac{\kappa a}{2}$ for all $\kappa > b$. □

3.4 Summary

Finally, let us summarize our findings concerning the spectrum of the operator H associated with the unperturbed comb:

Theorem 3.4.1: *Let* Γ *be the infinite comb introduced in Section 2.4. Let* H *denote the negative Laplacian acting on* $L^2(\Gamma)$ *according to* (2.1) *with the domain restricted by the vertex conditions* (2.3a)–(2.3c) *and* (2.4) *on the assumption that* $\beta \neq 0$. *Then the spectrum of* H *is bounded from below and consists of an infinite number of spectral bands separated by open intervals. The positive part of the continuous spectrum of* H *is formed by* k^2, $k > 0$, *such that*

$$\left| \cos ka + \frac{\sin ka}{2} \left(\frac{\delta}{k} + \frac{\beta^2 \cos kc}{\sin kc + k\gamma \cos kc} \right) \right| \leq 1.$$

0 belongs to the spectrum of H *if and only if*

$$\left| 1 + \frac{a}{2} \left(\delta + \frac{\beta^2}{c+\gamma} \right) \right| \leq 1.$$

The negative part of the continuous spectrum comprises $-\kappa^2$, $\kappa > 0$, *satisfying*

$$\left| \cosh \kappa a + \frac{\sinh \kappa a}{2} \left(\frac{\delta}{\kappa} + \frac{\beta^2 \cosh \kappa c}{\sinh \kappa c + \kappa\gamma \cosh \kappa c} \right) \right| \leq 1$$

and is nonempty if and only if

$$\gamma \in [-c,\, 0) \vee \delta + \frac{\beta^2}{c+\gamma} < 0.$$

The only eigenvalues in the spectrum of H *are the degenerated spectral bands arising at* k^2, $k > 0$, *such that*

$$k \in \left\{ \frac{m\pi}{a} | m \in \mathbb{N} \right\} \quad \wedge \quad \sin kc + k\gamma \cos kc = 0.$$

Chapter 4

Local perturbation

In this chapter we will introduce a local perturbation into the comb studied in Chapter 3: we select one of the teeth and change its length to c_*. At the same time, we consider a simultaneous modification of the parameters defining the boundary conditions at the vertex where the tooth is attached to the straight line. The question is how such modifications affect the spectrum. We will derive relations determining the positions of newly arising eigenvalues and then examine the case of a simple tooth prolongation without changing the vertex conditions in more detail. As for the notation, we assign a 0-index to the perturbed tooth; the remaining teeth are denoted by nonzero integer indices (positive or negative, see Fig. 4.1).

The boundary conditions imposed on each vertex on the straight line except the zeroth one are given by (2.3a)–(2.3c); the boundary conditions

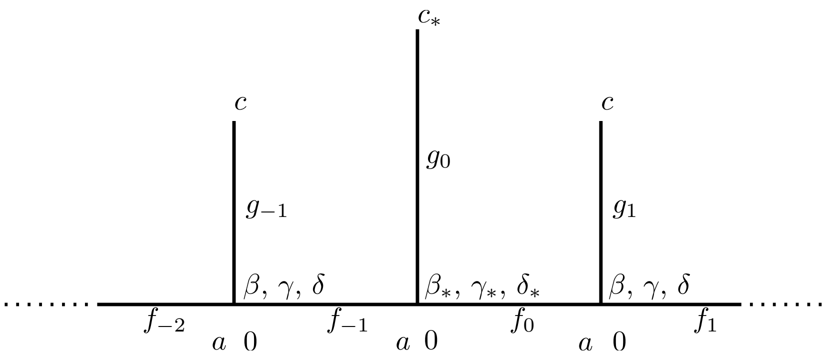

Figure 4.1: The infinite comb after perturbation

with modified parameter values at the zeroth vertex are

$$f_0(0) = f_{-1}(a) \tag{4.1a}$$
$$g_0(0) = \beta_* f_{-1}(a) + \gamma_* g_0'(0+) \tag{4.1b}$$
$$f_0'(0+) - f_{-1}'(a-) = \delta_* f_{-1}(a) - \beta_* g_0'(0+). \tag{4.1c}$$

In addition, the wavefunction must satisfy (2.4) at the ends of the teeth with nonzero indices and

$$g_0(c_*) = 0 \tag{4.2}$$

on the zeroth tooth.

Due to the symmetry of both the comb and the vertex conditions, the perturbed Hamiltonian H_* can be decomposed into the direct sum of an even part H_*^+ and an odd part H_*^-. As a result, when looking for eigenfunctions of H_*, we can restrict ourselves to even/odd quadratically integrable functions defined on the graph. This makes our considerations easier since we need to inspect the quadratic integrability of the wavefunction on the part of the graph with positive indices only; the quadratic integrability on the part with negative indices is then guaranteed by the symmetry.

4.1 General case

4.1.1 Positive part of the spectrum

Let us assume that $k > 0$. The Ansatz for f_p, g_p, $p \in \mathbb{N}$ can be chosen as follows:

$$f_p(x) = R_p(k)\cos kx + S_p(k)\sin kx, \quad x \in [0,\, a],\ R_p(k), S_p(k) \in \mathbb{C}$$
$$g_p(x) = T_p(k)\cos kx + U_p(k)\sin kx, \quad x \in [0,\, c],\ T_p(k), U_p(k) \in \mathbb{C}.$$

Analogously, the Ansatz for f_0, g_0 is

$$f_0(x) = R_0(k)\cos kx + S_0(k)\sin kx, \quad x \in [0,\, a],\ R_0(k), S_0(k) \in \mathbb{C}$$
$$g_0(x) = T_0(k)\cos kx + U_0(k)\sin kx, \quad x \in [0,\, c_*],\ T_0(k), U_0(k) \in \mathbb{C}.$$

Transition matrix and integrability Let us first consider the case $k > 0$, $\sin kc + k\gamma\cos kc \neq 0$. From the vertex conditions (2.3a)–(2.3c) and (2.4) we obtain the following relation between the coefficients belonging to f_p and f_{p+1}, $p \in \mathbb{N}_0$

$$\begin{pmatrix} R_{p+1}(k) \\ S_{p+1}(k) \end{pmatrix} = M(k) \cdot \begin{pmatrix} R_p(k) \\ S_p(k) \end{pmatrix} = M^{p+1}(k) \cdot \begin{pmatrix} R_0(k) \\ S_0(k) \end{pmatrix}, \tag{4.5}$$

where $M(k)$ is a transition matrix[1] of the shape

$$M(k) = \begin{pmatrix} \cos ka & \sin ka \\ -\sin ka + A(k)\cos ka & \cos ka + A(k)\sin ka \end{pmatrix}. \tag{4.6}$$

Based on the knowledge of $R_p(k)$ and $S_p(k)$, the (p+1)th-tooth coefficients can be computed as

$$\begin{pmatrix} T_{p+1}(k) \\ U_{p+1}(k) \end{pmatrix} = \frac{\beta}{\sin kc + k\gamma\cos kc} \begin{pmatrix} \sin kc\cos ka & \sin kc\sin ka \\ -\cos kc\cos ka & -\cos kc\sin ka \end{pmatrix} \cdot \begin{pmatrix} R_p(k) \\ S_p(k) \end{pmatrix} \tag{4.7}$$

The eigenvalues of the matrix $M(k)$ defined in (4.6) are determined by the equation

$$0 = \lambda^2 - 2B(k)\lambda + 1, \tag{4.8}$$

where $B(k)$ stands for

$$B(k) = \cos ka + \frac{\sin ka}{2} A(k),$$

which is nothing but the expression that defines positive spectral bands in the unperturbed case. The solutions of the characteristic equation (4.8) are

$$\lambda_\pm(k) = B(k) \pm \sqrt{B^2(k) - 1}$$

and the corresponding eigenvectors can be selected as

$$v_\pm(k) = \begin{pmatrix} \sin ka \\ \lambda_\pm(k) - \cos ka \end{pmatrix}$$

provided $k \neq \frac{m\pi}{a}$, $m \in \mathbb{N}$, or

$$v_\pm(k) = \begin{pmatrix} 0 \\ 1 \end{pmatrix}$$

if $k = \frac{m\pi}{a}$, $m \in \mathbb{N}$. It is important to note that $\lambda_+(k)\lambda_-(k) = 1$. Therefore, $\lambda_+(k)$, $\lambda_-(k)$ may either be two complex conjugate numbers with modulus equal to 1, or two real numbers with the same sign, one of them having an absolute value strictly greater than 1, the other strictly lower than 1. Let us consider an eigenfunction of $H^\pm$ corresponding to k^2, $k > 0$, with coefficients $(R_0(k),\ S_0(k))^T$ determining the component f_0. Since the eigenfunction is quadratically integrable, from transition relations (4.5) and (4.7) it follows

[1] Please note that the term transition matrix used here should not be confused with the notion of a transfer matrix used in the theory of ODE.

that $(R_0(k),\ S_0(k))^T$ must either be a zero vector or an eigenvector corresponding to that real eigenvalue of $M(k)$ which has a modulus strictly lower than 1. Consequently, if k^2 is an eigenvalue of $H^{\pm}$, $|B(k)|$ must be strictly greater than 1. If $B(k) > 1$, $(R_0(k),\ S_0(k))^T$ is zero or an eigenvector corresponding to $\lambda_-(k)$; if $B(k) < -1$, $(R_0(k),\ S_0(k))^T$ corresponds to $\lambda_+(k)$. Conversely, if $(R_0(k),\ S_0(k))^T$ is an eigenvector of $M(k)$ corresponding to that eigenvalue of $M(k)$ with an absolute value lower than 1, and the boundary conditions at the zeroth vertex are satisfied, the resulting wavefunction is an eigenfunction of $H^{\pm}$.

The case of $M(k)$ having two complex conjugate eigenvalues, which occurs if and only if $|B(k)| \leq 1$, implies that k^2 belongs to the continuous spectrum of $H^{\pm}$.

Finally, let us mention how the character of wavefunctions is restricted by the boundary conditions (2.3a)–(2.3c) and (2.4) in the case of $\sin kc + k\gamma \cos kc = 0$:

Lemma 4.1.1: *Let $k > 0$, $\sin kc + k\gamma \cos kc = 0$. Then $R_p(k) = S_p(k) = 0$ for all $p \in \{1, 2, \dots\}$ and $T_p(k) = U_p(k) = 0$ for all $p \in \{2, 3, \dots\}$.*

Proof. First, we will treat the case $\gamma = 0$: we have $\sin kc = 0$, therefore, from (2.4) it follows that $T_p(k) = 0$ for all $p \in \mathbb{Z}$. From (2.3b) one gets that $R_p(k) = 0$ for all $p \in \mathbb{N}$, and by taking this into account, from (2.3a) one infers that $S_p(k) = 0$ for all $p \in \mathbb{N}$ as well. The condition (4.1c) then gives the statement $U_p(k) = 0$ for all $p \in \{2, 3, \dots\}$.

The case $\gamma \neq 0$ can be treated similarly to the previous one: using the condition (2.4), one expresses $U_{p+1}(k)$ as $U_{p+1}(k) = -\cot kc \cdot T_{p+1}(k)$, and by substituting this into the condition (2.3b), one gets that $R_p(k) = 0$ for all $p \in \mathbb{N}$ again. The remaining considerations are the same as in the previous case. $\square$

Spectrum of $\mathbf{H}_*^+$ We will now consider wavefunctions even with respect to the axis containing the zeroth tooth. This implies that $f_{-1}(a) = f_0(0)$ and $f'_{-1}(a-) = -f'_0(0+)$. As a result, the boundary conditions (4.1a)-(4.2) at the vertex to which the zeroth tooth is attached become

$$f_{-1}(a) = f_0(0) \tag{4.9a}$$
$$g_0(0) = \beta_* f_0(0) + \gamma_* g'_0(0+) \tag{4.9b}$$
$$2f'_0(0+) = \delta_* f_0(0) - \beta_* g'_0(0+), \tag{4.9c}$$
$$g_0(c_*) = 0. \tag{4.9d}$$

As we have already suggested, we are going to forget about the part of the graph with negative indices and see how the conditions (4.9b)–(4.9d) affect the choice of $(R_0(k),\ S_0(k))^T$:

Lemma 4.1.2: *Let $k > 0$. The coefficient vector $(R_0(k),\ S_0(k))^T$ of every eigenfunction of H_*^+ corresponding to k^2 is a multiple of*

- $(1,\ A_*(k)/2)^T$ *– if* $\sin kc_* + k\gamma_* \cos kc_* \neq 0$,
- $(0,\ 1)^T$ *– if* $\sin kc_* + k\gamma_* \cos kc_* = 0$,

where $A_*(k) = \frac{\delta_*}{k} + \frac{\beta_*^2 \cos kc_*}{\sin kc_* + k\gamma_* \cos kc_*}$.

This lemma, which can easily be verified, will help us prove the following proposition dealing with positive eigenvalues of H_*^+:

Proposition 4.1.1: (Positive eigenvalues of H_*^+)
Let $k > 0$ and $\sin kc_* + k\gamma_* \cos kc_* \neq 0$*:*

- *Given* $\sin kc + k\gamma \cos kc \neq 0$*, then k^2 is an eigenvalue of H_*^+ if and only if*
$$|B(k)| > 1 \quad \wedge \quad B_*(k) = B(k) - \operatorname{sgn}(B(k))\sqrt{B^2(k) - 1},$$
where $B_*(k) = \cos ka + \frac{\sin ka}{2}\left(\frac{\delta_*}{k} + \frac{\beta_*^2 \cos kc_*}{\sin kc_* + k\gamma_* \cos kc_*}\right) = \cos ka + \frac{\sin ka}{2} A_*(k)$.
- *Provided* $\sin kc + k\gamma \cos kc = 0$*, k^2 is an eigenvalue of H_*^+ if and only if*
$$B_*(k) = 0.$$

Let $k > 0$ and $\sin kc_* + k\gamma_* \cos kc_* = 0$. Then k^2 is an eigenvalue of H_*^+ if and only if $\sin kc + k\gamma \cos kc = 0$ and $k = \frac{m\pi}{a}$, $m \in \mathbb{N}$.

Proof. Let us first prove the case $\sin kc_* + k\gamma_* \cos kc_* \neq 0$. According to Lemma 4.1.2, we can put $(R_0(k),\ S_0(k))^T = (1,\ A_*(k)/2)^T$. Since we need the absolute value of one of $\lambda_\pm(k)$ to be strictly lower than 1, we can exclude the case $k = \frac{m\pi}{a}$, $m \in \mathbb{N}$. Consequently, $(R_0(k),\ S_0(k))^T$ is a multiple of $v_\pm(k)$, the eigenvector of the matrix $M(k)$, if and only if

$$0 = \begin{vmatrix} \sin ka & 1 \\ \frac{A(k)}{2}\sin ka \pm \sqrt{\left(\frac{A^2(k)}{4} - 1\right)\sin^2 ka + A(k)\sin ka \cos ka} & \frac{A_*(k)}{2} \end{vmatrix},$$

which can be rewritten as

$$B_*(k) = B(k) \pm \sqrt{B^2(k) - 1}.$$

The rest follows from our previous considerations.

In the case of $\sin kc + k\gamma\cos kc = 0$, we will make use of Lemma 4.1.1. From the condition (2.3a) we obtain $0 = R_1(k) = \cos ka + \frac{A_*(k)}{2}\sin ka = B_*(k)$, which yields a necessary condition for the existence of an eigenvalue, and from (2.3c) we get that

$$U_1(k) = \frac{1}{\beta}\left(-R_0(k)\sin ka + S_0(k)\cos ka\right) = \frac{1}{\beta}\left(-\sin ka + \frac{A_*(k)}{2}\cos ka\right).$$

Conversely, if $B_*(k) = 0$, we can construct an eigenfunction of H_*^+ as an even wavefunction with a compact support such that
$R_0(k) = 1$, $S_0(k) = \frac{A_*(k)}{2}$, $T_0(k) = \frac{\beta_*\sin kc_*}{\sin kc_* + k\gamma_*\cos kc_*}$, $U_0(k) = -\frac{\beta_*\cos kc_*}{\sin kc_* + k\gamma_*\cos kc_*}$, $T_1(k) = \frac{-\tan kc}{\beta}\left(-\sin ka + \frac{A_*(k)}{2}\cos ka\right)$, $U_1(k) = \frac{1}{\beta}\left(-\sin ka + \frac{A_*(k)}{2}\cos ka\right)$, $R_p(k) = S_p(k) = 0$ for all $p \in \{1, 2, \dots\}$ and $T_p(k) = U_p(k) = 0$ for all $p \in \{2, 3, \dots\}$.

Let us mention the case $\sin kc_* + k\gamma_*\cos kc_* = 0$. The coefficient vector $(R_0(k),\ S_0(k))^T$ can now be selected as $(R_0(k),\ S_0(k))^T = (0,\ 1)^T$. Assuming that $\sin kc + k\gamma\cos kc \neq 0$, $(R_0(k),\ S_0(k))^T$ is a multiple of $v_\pm(k)$ if and only if

$$0 = \begin{vmatrix} \sin ka & 0 \\ \frac{A(k)}{2}\sin ka \pm \sqrt{\left(\frac{A(k)^2}{4} - 1\right)\sin^2 ka + A(k)\sin ka\cos ka} & 1 \end{vmatrix}.$$

This can be rewritten simply as

$$0 = \sin ka.$$

Since we have excluded $k = \frac{m\pi}{a}$, this condition is never satisfied. If $\sin kc + k\gamma\cos kc = 0$, from Lemma 4.1.1 we get a necessary condition $0 = R_1 = \sin ka$. On the other hand, if $k = \frac{m\pi}{a}$, $m \in \mathbb{N}$, we can construct an eigenfunction of H_*^+ by putting $R_0(k) = 0$, $S_0(k) = 1$, $T_0(k) = \frac{2\tan kc_*}{\beta_*}$, $U_0(k) = -\frac{2}{\beta_*}$, $T_1(k) = \frac{-\tan kc}{\beta}\cos ka$, $U_1(k) = \frac{1}{\beta}\cos ka$, $R_p(k) = S_p(k) = 0$ for all $p \in \{1, 2, \dots\}$ and $T_p(k) = U_p(k) = 0$ for all $p \in \{2, 3, \dots\}$. $\square$

Spectrum of $\mathbf{H}_*^-$ Let us focus our attention on the odd part of the perturbed Hamiltonian. We require that $f_0(0) = 0$, $g_0(x) = 0$ for all $x \in [0, c_*]$ and $f'_{-1}(a-) = f'_0(0+)$. It is easy to verify that the following lemma holds:

Lemma 4.1.3: *Let $k > 0$. The coefficient vector $(R_0(k),\ S_0(k))^T$ of every eigenfunction of H_*^- corresponding to k^2 is a multiple of $(0,\ 1)^T$.*

Using this lemma, we obtain the following statement:

Proposition 4.1.2: (Eigenvalues of H_*^-) *Let $k > 0$, then k^2 is an eigenvalue of H_*^- if and only if*

$$\sin kc + k\gamma \cos kc = 0 \quad \wedge \quad k \in \frac{m\pi}{a},\ m \in \mathbb{N}.$$

Proof. From Lemma 4.1.3 it follows that we can put $(R_0(k),\ S_0(k))^T = (0,\ 1)$.

Let $\sin kc + k\gamma \cos kc \neq 0$. By using the same reasoning as in Proposition 4.1.1 for $\sin kc_* + k\gamma_* \cos kc_* = 0$ and $\sin kc + k\gamma \cos kc \neq 0$, we see that there is no possibility of H_*^- having an eigenvalue in this case.

On the other hand, if $\sin kc + k\gamma \cos kc = 0$, we find out that k^2 is an eigenvalue of H_*^- if and only if $\sin ka = 0$ (again in the same way as in Proposition 4.1.1, now for $\sin kc_* + k\gamma_* \cos kc_* = 0$ and $\sin kc + k\gamma \cos kc = 0$). The coefficients of the corresponding odd eigenfunction are $R_0(k) = 0$, $S_0(k) = 1$, $T_0(k) = 0$, $U_0(k) = 0$, $T_1(k) = \frac{-\tan kc}{\beta} \cos ka$, $U_1(k) = \frac{1}{\beta} \cos ka$, $R_p(k) = S_p(k) = 0$ for all $p \in \{1, 2, \dots\}$ and $T_p(k) = U_p(k) = 0$ for all $p \in \{2, 3, \dots\}$. $\square$

4.1.2 Zero and negative part of the spectrum

First, let us inspect the case $k = 0$. The Ansatz of the wavefunction components can now be chosen as

$$\begin{aligned} f_p(x) &= R_p(0) + S_p(0)x, \quad x \in [0,\ a],\ R_p(0), S_p(0) \in \mathbb{C} \\ g_p(x) &= T_p(0) + U_p(0)x, \quad x \in [0,\ c],\ T_p(0), U_p(0) \in \mathbb{C} \end{aligned}$$

for $p \in \mathbb{N}$ and

$$\begin{aligned} f_0(x) &= R_0(0) + S_0(0)x, \quad x \in [0,\ a],\ R_0(0), S_0(0) \in \mathbb{C} \\ g_0(x) &= T_0(0) + U_0(0)x, \quad x \in [0,\ c_*],\ T_0(0), U_0(0) \in \mathbb{C} \end{aligned}$$

on the zeroth tooth.

Provided $\gamma \neq -c$ we can construct a transition matrix $M(0)$ similar to $M(k)$ for the positive part of the spectrum:

$$\begin{pmatrix} R_{p+1}(0) \\ S_{p+1}(0) \end{pmatrix} = M(0) \cdot \begin{pmatrix} R_p(0) \\ S_p(0) \end{pmatrix} = M^{p+1}(0) \cdot \begin{pmatrix} R_0(0) \\ S_0(0) \end{pmatrix},$$

where $M(0)$ is defined as

$$M(0) = \begin{pmatrix} 1 & a \\ A(0) & 1 + A(0)a \end{pmatrix}, \qquad A(0) = \delta + \frac{\beta^2}{c + \gamma}.$$

Again, we can look at the eigenvalues of the matrix $M(0)$ determined by the equation

$$0 = \lambda^2 - 2B(0)\lambda + 1, \tag{4.12}$$

where $B(0)$ is now defined as

$$B(0) = 1 + \frac{a}{2}A(0) = 1 + \frac{a}{2}\left(\delta + \frac{\beta^2}{c+\gamma}\right).$$

Like in the positive case, the characteristic equation (4.12) has two solutions

$$\lambda_\pm(0) = B(0) \pm \sqrt{(B(0))^2 - 1},$$

either two complex conjugates with modulus one, or two real solutions of the same sign, one of them having an absolute value strictly greater than 1, the other strictly lower than 1. The eigenvectors of $M(0)$ corresponding to $\lambda_\pm(0)$ are nonzero multiples of

$$v_\pm(0) = \begin{pmatrix} a \\ \lambda_\pm(0) - 1 \end{pmatrix}.$$

On the other hand, if $\gamma = -c$, we get the following lemma (analogous to Lemma 4.1.1)

Lemma 4.1.4: *Let $k = 0$, $\gamma = -c$. Then $R_p(0) = S_p(0) = 0$ for all $p \in \{1, 2, \dots\}$ and $T_p(0) = U_p(0) = 0$ for all $p \in \{2, 3, \dots\}$.*

For H_*^+, the even part of the perturbed Hamiltonian, the following lemma (a slight modification of Lemma 4.1.2) holds:

Lemma 4.1.5: *Let $k = 0$. The coefficient vector $(R_0(0),\ S_0(0))^T$ of every eigenfunction of H_*^+ corresponding to 0 is a multiple of*

- $(1,\ A_*(0)/2)^T$ *– if $\gamma_* \neq -c_*$,*
- $(0,\ 1)^T$ *– if $\gamma_* = -c_*$,*

where $A_*(0) = \delta_* + \frac{\beta_*^2}{\gamma_*+c_*}$.

Now, we can formulate the necessary and sufficient condition for 0 to be an eigenvalue of H_*^+:

Proposition 4.1.3: (0 as an eigenvalue of H_*^+)
Let $\gamma_* \neq -c_*$:

- *Given $\gamma \neq -c$, 0 is an eigenvalue of H_*^+ if and only if*

$$|B(0)| > 1 \quad \wedge \quad B_*(0) = B(0) - \operatorname{sgn}(B(0))\sqrt{(B^2(0)) - 1},$$

  where $B_*(0) = 1 + \frac{a}{2}A_*(0) = 1 + \frac{a}{2}\left(\delta_* + \frac{\beta_*^2}{c_*+\gamma_*}\right)$.

- *Provided $\gamma = -c$, 0 is an eigenvalue of H_*^+ if and only if*

$$B_*(0) = 0.$$

Let $\gamma_* = -c_*$. Then 0 is not an eigenvalue of H_*^+.

The proof of this proposition is analogous to that of Proposition 4.1.1, dealing with positive eigenvalues of H_*^+.

As for the odd part H_*^- of the perturbed Hamiltonian, we find out that, for every eigenfunction of H_*^- corresponding to 0, $(R_0(0),\ S_0(0))^T$ must be a multiple of $(0,\ 1)^T$. Analogously to the previous cases, it is then easy to verify that:

Proposition 4.1.4: *0 is not an eigenvalue of H_*^-.*

The negative parts of the point spectra of H_*^+ and H_*^- can be examined simply by putting $k = i\kappa$ and using the relations derived for $k > 0$. The expression $A(k)$ then transforms into $A(i\kappa) = -i\left(\frac{\delta}{\kappa} + \frac{\beta^2 \cosh \kappa c}{\sinh \kappa c + \kappa\gamma \cosh \kappa c}\right) := -i\tilde{A}(\kappa)$ and $B(i\kappa) = \cosh \kappa a + \frac{\tilde{A}(\kappa)}{2} \sinh \kappa a := \tilde{B}(\kappa)$. The following two propositions describe the results concerning the negative eigenvalues of H_*^+ and H_*^-:

Proposition 4.1.5: (Negative eigenvalues of H_*^+)
Let $\kappa > 0$ and $\sinh \kappa c_* + \kappa\gamma_* \cos \kappa c_* \neq 0$:

- *Given $\sinh \kappa c + \kappa\gamma \cosh \kappa c \neq 0$, then $-\kappa^2$ is an eigenvalue of H_*^+ if and only if*

$$|\tilde{B}(\kappa)| > 1 \quad \wedge \quad \tilde{B}_*(\kappa) = \tilde{B}(\kappa) - \operatorname{sgn}(\tilde{B}(\kappa))\sqrt{\tilde{B}^2(\kappa) - 1},$$

  where $\tilde{B}_*(\kappa) = \cosh \kappa a + \frac{\sinh \kappa a}{2}\left(\frac{\delta_*}{\kappa} + \frac{\beta_*^2 \cosh \kappa c_*}{\sinh \kappa c_* + \kappa\gamma_* \cosh \kappa c_*}\right) = \cosh \kappa a + \frac{\sinh \kappa a}{2}\tilde{A}_*(\kappa)$.

- *Provided $\sinh \kappa c + \kappa\gamma \cosh \kappa c = 0$, $-\kappa^2$ is an eigenvalue of H_*^+ if and only if*

$$\tilde{B}_*(\kappa) = 0.$$

Let $\kappa > 0$ and $\sinh \kappa c_* + \kappa\gamma_* \cosh \kappa c_* = 0$. Then $-\kappa^2$ is not an eigenvalue of H_*^+.

Proposition 4.1.6: *H_*^- has no negative eigenvalues.*

4.1.3 Summary

Before we summarize our findings regarding the eigenvalues arising after a local perturbation, let us remark that if we use Proposition 4.1.1, putting $\beta_* = \beta$, $\gamma_* = \gamma$, $\delta_* = \delta$, $c_* = c$, and Proposition 4.1.2, we get that in the case of the unperturbed comb, every k^2, $k > 0$, satisfying

$$\sin kc + k\gamma \cos kc = 0 \quad \wedge \quad k \in \frac{m\pi}{a},\ m \in \mathbb{N}$$

is an eigenvalue of both H^+ and H^-. If we transform the corresponding eigenfunctions introduced in those two propositions according to (3.1)–(3.3), we obtain the two functions $\varphi(\theta, .) = \{\varphi_L(\theta, .),\ \varphi_R(\theta, .),\ \varphi_T(\theta, .)\}$ used in Proposition 3.2.3 to prove that such a k^2 is an eigenvalue of $H(\theta)$ for all $\theta \in [-\pi, \pi)$ and therefore, an eigenvalue of H itself.

Finally, let us formulate a theorem summarizing the information obtained about the spectrum of the Hamiltonian after a local perturbation:

Theorem 4.1.1: *Let H_* be the perturbed Hamiltonian introduced at the beginning of this chapter. The continuous spectrum of H_* remains the same as in the unperturbed case. The same holds for the eigenvalues k^2, $k > 0$, such that $\sin kc + k\gamma \cos kc = 0$ and $k \in \left\{\frac{m\pi}{a} | m \in \mathbb{N}\right\}$.*

However, in contrast to the unperturbed case, new eigenvalues may emerge in spectral gaps. In the positive part of the spectrum, these eigenvalues are given as k^2, $k > 0$, where k satisfies $\sin kc_* + k\gamma_* \cos kc_* \neq 0$ and is a solution of

$$B_*(k) = B(k) - \operatorname{sgn}(B(k))\sqrt{B^2(k) - 1}. \tag{4.13}$$

Provided $\sin kc + k\gamma \cos kc \neq 0$, $B(k)$ is defined as

$$B(k) = \cos ka + \frac{\sin ka}{2}\left(\frac{\delta}{k} + \frac{\beta^2 \cos kc}{\sin kc + k\gamma \cos kc}\right).$$

$B_*(k)$ has the same shape as $B(k)$, but with β_*, γ_* and δ_* in place of β, γ and δ. If $\sin kc + k\gamma \cos kc = 0$, the right-hand side of (4.13) is replaced by

$$0 = \lim_{x \to k}\left(B(x) - \operatorname{sgn}(B(x))\sqrt{B^2(x) - 1}\right).$$

0 is an eigenvalue of H_* if and only if $\gamma_* \neq -c_*$ and the following condition holds

$$B_*(0) = B(0) - \operatorname{sgn}(B(0))\sqrt{(B^2(0)) - 1}. \tag{4.14}$$

If $\gamma \neq -c$, $B(0)$ is defined as

$$B(0) = \lim_{x \to 0+} B(x) = 1 + \frac{a}{2}\left(\delta + \frac{\beta^2}{c+\gamma}\right).$$

Again, $B_*(0)$ has the same shape as $B(0)$, but with β_*, γ_* and δ_* in place of β, γ and δ. If $c = -\gamma$, the right-hand side of (4.14) is replaced by 0. The negative eigenvalues $-\kappa^2$, $\kappa > 0$, satisfy $\sinh \kappa c_* + \kappa\gamma_* \cosh \kappa c_* \neq 0$ and are solutions of the equation

$$\tilde{B}_*(\kappa) = \tilde{B}(\kappa) - \operatorname{sgn}(\tilde{B}(\kappa))\sqrt{\tilde{B}^2(\kappa) - 1}. \tag{4.15}$$

If $\sinh \kappa c + \kappa\gamma \cosh \kappa c \neq 0$, $\tilde{B}(\kappa)$ reads

$$\tilde{B}(\kappa) = \cosh \kappa a + \frac{\sinh \kappa a}{2}\left(\frac{\delta}{\kappa} + \frac{\beta^2 \cosh \kappa c}{\sinh \kappa c + \kappa\gamma \cosh \kappa c}\right)$$

and $\tilde{B}_*(\kappa)$ has the same shape, but with β_*, γ_* and δ_* instead of β, γ and δ. If $\sinh \kappa c + \kappa\gamma \cosh \kappa c = 0$, the right-hand side of (4.15) becomes

$$0 = \lim_{x \to \kappa}\left(\tilde{B}(x) - \operatorname{sgn}(\tilde{B}(x))\sqrt{\tilde{B}^2(x) - 1}\right).$$

4.2 Tooth prolongation

Now we will deal with a special case of the local perturbation studied above: we take one of the teeth and simply increase its length from c to $c_* > c$. The lengths of the other teeth remain the same as in the unperturbed system, and $\beta_* = \beta$, $\gamma_* = \gamma$ and $\delta_* = \delta$.

Let us a consider a spectral gap (p_1^2, p_2^2), $p_1 \geq 0$, $p_2 > 0$, situated in the positive part of the spectrum. The eigenvalues k^2, $k > 0$, potentially present in the spectral gap, are given by solutions of the following equation (4.13):

$$B_*(k) = B(k) - \operatorname{sgn}(B(k))\sqrt{B^2(k) - 1}.$$

For $k \in (p_1, p_2)$, the right-hand side belongs to $(0, 1)$ if $B(k) > 1$, and $(-1, 0)$ if $B(k) < -1$. On the edges of the spectral bands, the right-hand side becomes:

$$B(p_{1,2}) - \operatorname{sgn}(B(p_{1,2}))\sqrt{B^2(p_{1,2}) - 1} = B(p_{1,2}) = \pm 1. \tag{4.16}$$

Furthermore, the first derivative of the right-hand side differs in sign from the first derivative of $B(.)$:

$$\operatorname{sgn}\left(B(k) - \operatorname{sgn}(B(k))\sqrt{B^2(k)-1}\right)' = -\operatorname{sgn} B'(k) \tag{4.17}$$

since

$$\left(B(k) - \operatorname{sgn}(B(k))\sqrt{B^2(k)-1}\right)' = \\ -\frac{B'(k)}{\sqrt{B^2(k)-1}}\operatorname{sgn}(B(k))\left(B(k) - \operatorname{sgn}(B(k))\sqrt{B^2(k)-1}\right).$$

While k^2 approaches the edges p_1^2 and p_2^2 which enclose the spectral gap, we notice that $\left(B(k) - \operatorname{sgn}(B(k))\sqrt{B^2(k)-1}\right)'$ goes to $\pm\infty$ – at least if $B'(k)$ does not tend to zero at the same time:

$$\lim_{k\to p_1+}\left(B(k) - \operatorname{sgn}(B(k))\sqrt{B^2(k)-1}\right)' = -\infty\cdot\operatorname{sgn} B(k), \tag{4.18}$$

$$\lim_{k\to p_2-}\left(B(k) - \operatorname{sgn}(B(k))\sqrt{B^2(k)-1}\right)' = +\infty\cdot\operatorname{sgn} B(k). \tag{4.19}$$

When looking for eigenvalues present in the spectral gap, we search for points where the graph of $B_*(.)$,

$$B_*(k) = \cos ka + \frac{\sin ka}{2}\left(\frac{\delta}{k} + \frac{\beta^2\cos kc_*}{\sin kc_* + k\gamma\cos kc_*}\right) = \cos ka + \frac{\sin ka}{2}A_*(k),$$

intersects that of $B(.) - \operatorname{sgn}(B(.))\sqrt{B^2(.)-1}$. An important thing to realize is that

$$\frac{\partial A_*}{\partial c_*}(k) = -\frac{k\beta^2}{(\sin kc_* + k\gamma\cos kc_*)^2} < 0 \tag{4.20}$$

for all $k > 0$ where $A_*(k)$ is defined. This means that while c_* is increased from its initial value c, $A_*(k)$ decreases for a fixed $k > 0$ until $\sin kc_* + k\gamma\cos kc_* = 0$.

Let us start with the initial length $c_* = c$ and increase it gradually. We suspect that some eigenvalues appear in the spectral gaps. Since H_*, the perturbed Hamiltonian, continuously depends on c_* via its domain, it is reasonable to expect that these eigenvalues start their trajectories on the edges of the spectral bands (including the degenerated ones) which form the original spectrum.

First, suppose that p^2 is an edge of a non-degenerated spectral band (i.e. $\sin pc + p\gamma\cos pc \neq 0$) such that $p \in \left\{\frac{m\pi}{a}\middle| m\in\mathbb{N}\right\}$. It holds that $B_*(p) =$

$B(p) = (-1)^m$ for all $c_* > c$ unless $\sin pc_* + p\gamma \cos pc_* = 0$. If we assume for convenience that $B'(p) \neq 0$, considering (4.17) and (4.18)–(4.19) we find that there must exist an $\epsilon > 0$ such that no eigenvalue originates in the neighborhood of p^2 for any $c_* \in (c,\, c+\epsilon)$.

Next, let q^2 be an edge of a non-degenerated spectral band satisfying $q \notin \left\{\frac{m\pi}{a} | m \in \mathbb{N}\right\}$. Using (4.20), we infer that $\frac{\partial B_*}{\partial c_*}(p) < 0$ if $\sin qa > 0$, and $\frac{\partial B_*}{\partial c_*}(p) > 0$ if $\sin qa < 0$. Hence, if $B(q) = 1$ and $\sin qa > 0$, we find (taking into account (4.16) and the continuous dependence of $B_*(k)$ on c_*) that there exists an $\epsilon > 0$ such that for all $c_* \in (c,\, c+\epsilon)$ the graph of $B_*(.)$ intersects that of $B(.) - \operatorname{sgn}(B(.))\sqrt{B^2(.) - 1}$, which implies the existence of an eigenvalue in a neighborhood of q^2. Analogously, the same is true for $B(q) = -1$ and $\sin qa < 0$. However, in the remaining cases, i.e. $B(q) = 1$ and $\sin qa < 0$ or $B(q) = -1$ and $\sin qa > 0$, we infer that there exists an $\epsilon > 0$ such that for all $c_* \in (c,\, c+\epsilon)$ no eigenvalue separates from the edge. This becomes evident if we rewrite the equation (4.13) as

$$\sin ka\,(A_*(k) - A(k)) = -2\operatorname{sgn}(B(k))\sqrt{B^2(k) - 1}$$

since we know that $A_*(k) - A(k)$ is negative on a neighborhood of q for all c_* belonging to some $(c,\, c+\epsilon)$. In short, we learn that there may be gaps in the positive part of the spectrum where an eigenvalue arises after an arbitrarily small increase of c_* above c, and others where no eigenvalue can be found while c_* being in a certain interval $(c,\, c+\epsilon)$.

On the other hand, let us remark that as one continues increasing the length c_* of the selected tooth, some eigenvalues ultimately appear in every positive gap, and what more, their number in each gap eventually goes to infinity. This is due to the growing number of infinite discontinuities of $B_*(.)$ in each gap, which make the graph of $B_*(.)$ cross that of $B(.) - \operatorname{sgn}(B(.))\sqrt{B^2(.) - 1}$ with an increasing frequency.

To visualize parts of band spectra for different parameters and the behavior of eigenvalues originating in spectral gaps, we have performed some numerical calculations using the relations derived so far. In Section 4.3 several examples of spectra exposed to modifications of vertex condition parameters at a single vertex can be found. Here we show the effects of prolonging a single tooth assuming four different combinations of vertex condition parameters. The initial geometry of the comb is characterized by the values $a = c = 1$, i.e. the lengths of the teeth are the same as their distances. At first place, one should notice how strongly the choice of vertex condition parameters β, γ and δ influences the spectrum. In the first two spectra, degenerated spectral bands can be found with energies equal to $(\pi/a)^2$ and $(2\pi/a)^2$, which are absent from the other two spectra. Moreover, in Figure 4.2 and Figure

4.4 one will recognize the presence of a negative spectral band, which is in accordance with the necessary and sufficient condition derived in Chapter 3. In Figure 4.4 two spectral gaps are present where, in agreement with our predictions above, no eigenvalues arise for c_* in a certain interval $(c,\, c+\epsilon)$. Finally, in the first two figures it can be clearly seen how the number of eigenvalues present in the gaps grows with an increasing c_*.

In the negative part of the spectrum, eigenvalues $-\kappa^2$ are given by solutions $\kappa > 0$ of the following equation (4.15):

$$\tilde{B}_*(\kappa) = \tilde{B}(\kappa) - \operatorname{sgn}(\tilde{B}(\kappa))\sqrt{\tilde{B}^2(\kappa) - 1}.$$

Again, it holds that in the spectral gaps the right-hand side belongs to $(0,\, 1)$ if $\tilde{B}(\kappa) > 1$, and to $(-1,\, 0)$ if $\tilde{B}(\kappa) < -1$, while together with $\tilde{B}(\kappa)$ it becomes equal to ± 1 on the edges of spectral bands. Analogously to the positive case, the first derivatives of $\tilde{B}(.)$ and $\tilde{B}(.) - \operatorname{sgn}(\tilde{B}(.))\sqrt{\tilde{B}^2(.) - 1}$ differ in sign:

$$\operatorname{sgn}\left(\tilde{B}(\kappa) - \operatorname{sgn}(\tilde{B}(\kappa))\sqrt{\tilde{B}^2(\kappa) - 1}\right)' = -\operatorname{sgn}\tilde{B}'(\kappa).$$

Concerning

$$\tilde{B}_*(\kappa) = \cosh\kappa a + \frac{\sinh\kappa a}{2}\left(\frac{\delta}{\kappa} + \frac{\beta^2\cosh\kappa c_*}{\sinh\kappa c_* + \kappa\gamma\cosh\kappa c_*}\right)$$

we get that

$$\frac{\partial\tilde{B}_*}{\partial c_*}(\kappa) < 0 \tag{4.21}$$

for all $\kappa > 0$ except for points of discontinuity, where $\sinh\kappa c_* + \kappa\gamma\cosh\kappa c_* = 0$.

Let us suppose that there exists at least one negative spectral band in the spectrum of H. Let $-p^2$, $p > 0$, denote the lowest edge of the lowest spectral band. Then $\tilde{B}(p) = \tilde{B}(p) - \operatorname{sgn}(\tilde{B}(p))\sqrt{\tilde{B}^2(p) - 1} = 1$, $\tilde{B}(\kappa) > 1$ and $\tilde{B}(\kappa) - \operatorname{sgn}(\tilde{B}(\kappa))\sqrt{\tilde{B}^2(\kappa) - 1} \in (0,\, 1)$ for all $-\kappa^2 \in (-\infty,\, -p^2)$. The limits as $-\kappa^2$ goes to $-\infty$ are

$$\lim_{\kappa\to\infty}\tilde{B}(\kappa) = +\infty, \quad \lim_{\kappa\to\infty}\left(\tilde{B}(\kappa) - \operatorname{sgn}(\tilde{B}(\kappa))\sqrt{\tilde{B}^2(\kappa) - 1}\right) = 0.$$

For a $c_* > c$, $\tilde{B}_*(.)$ may have a discontinuity at a $\kappa \in (p,\, +\infty)$. In this case, from our considerations in 3.3.1 it follows that $(0,\, 1) \in \tilde{B}_*((p,\, +\infty))$. This in

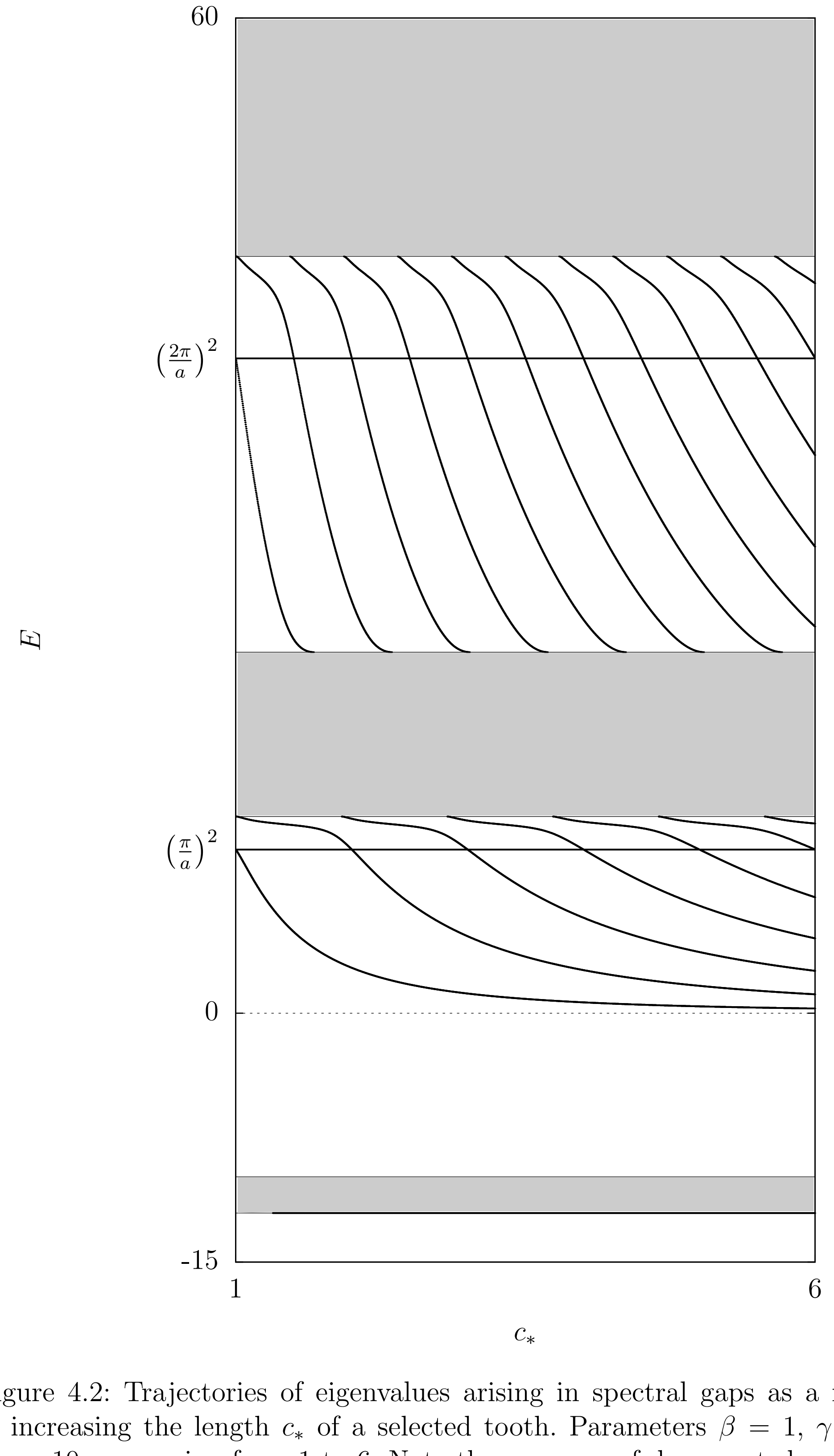

Figure 4.2: Trajectories of eigenvalues arising in spectral gaps as a result of increasing the length c_* of a selected tooth. Parameters $\beta = 1$, $\gamma = 0$, $\delta = -10$; c_* ranging from 1 to 6. Note the presence of degenerated spectral bands at $E = (\pi/a)^2$ and $E = (2\pi/a)^2$.

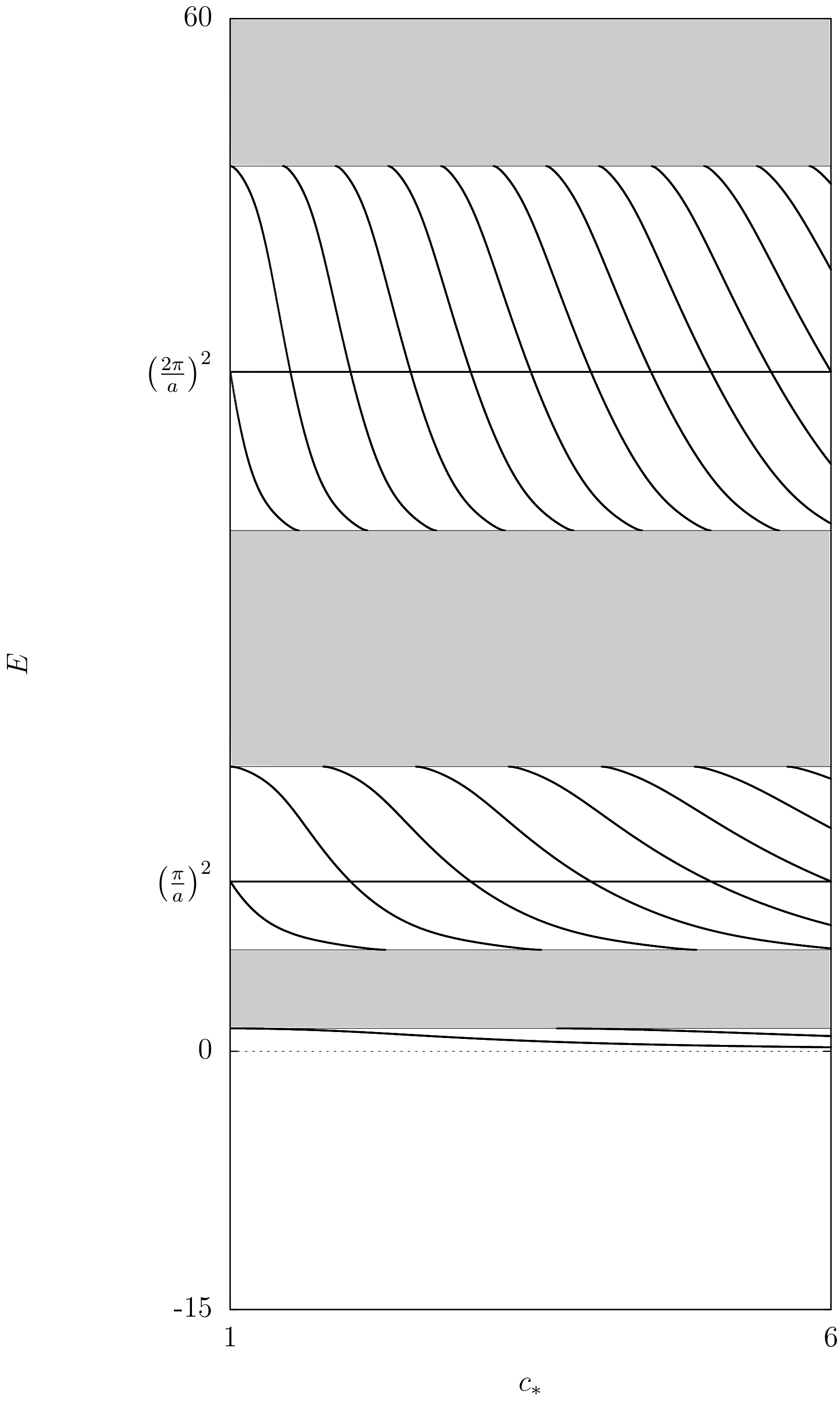

Figure 4.3: Trajectories of eigenvalues arising in spectral gaps as a result of increasing the length c_* of a selected tooth. Parameters $\beta = 1$, $\gamma = 0$, $\delta = 1$; c_* ranging from 1 to 6. Note the presence of degenerated spectral bands at $E = (\pi/a)^2$ and $E = (2\pi/a)^2$.

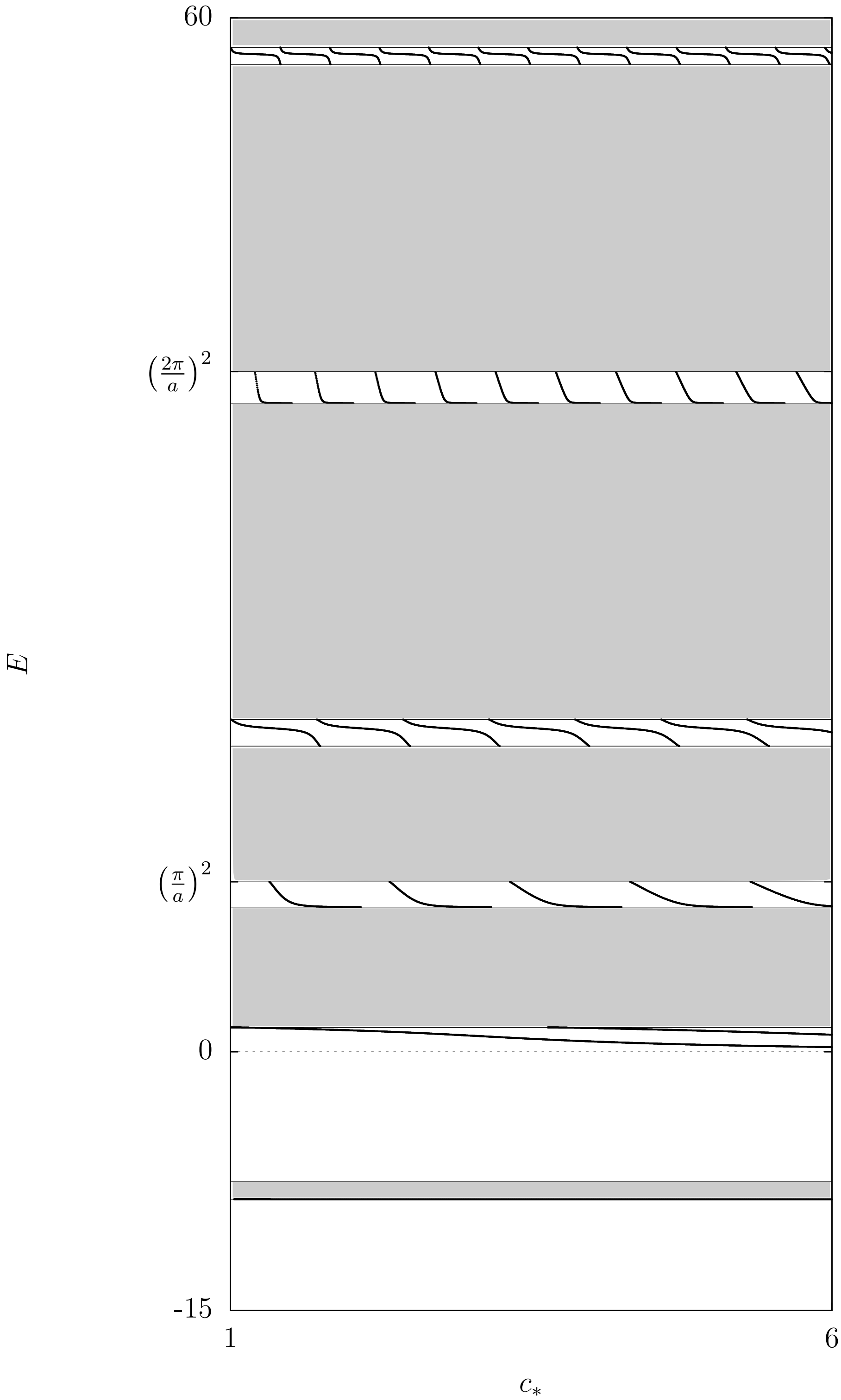

Figure 4.4: Trajectories of eigenvalues arising in spectral gaps as a result of increasing the length c_* of a selected tooth. Parameters $\beta = 1$, $\gamma = -0.5$, $\delta = 1$; c_* ranging from 1 to 6.

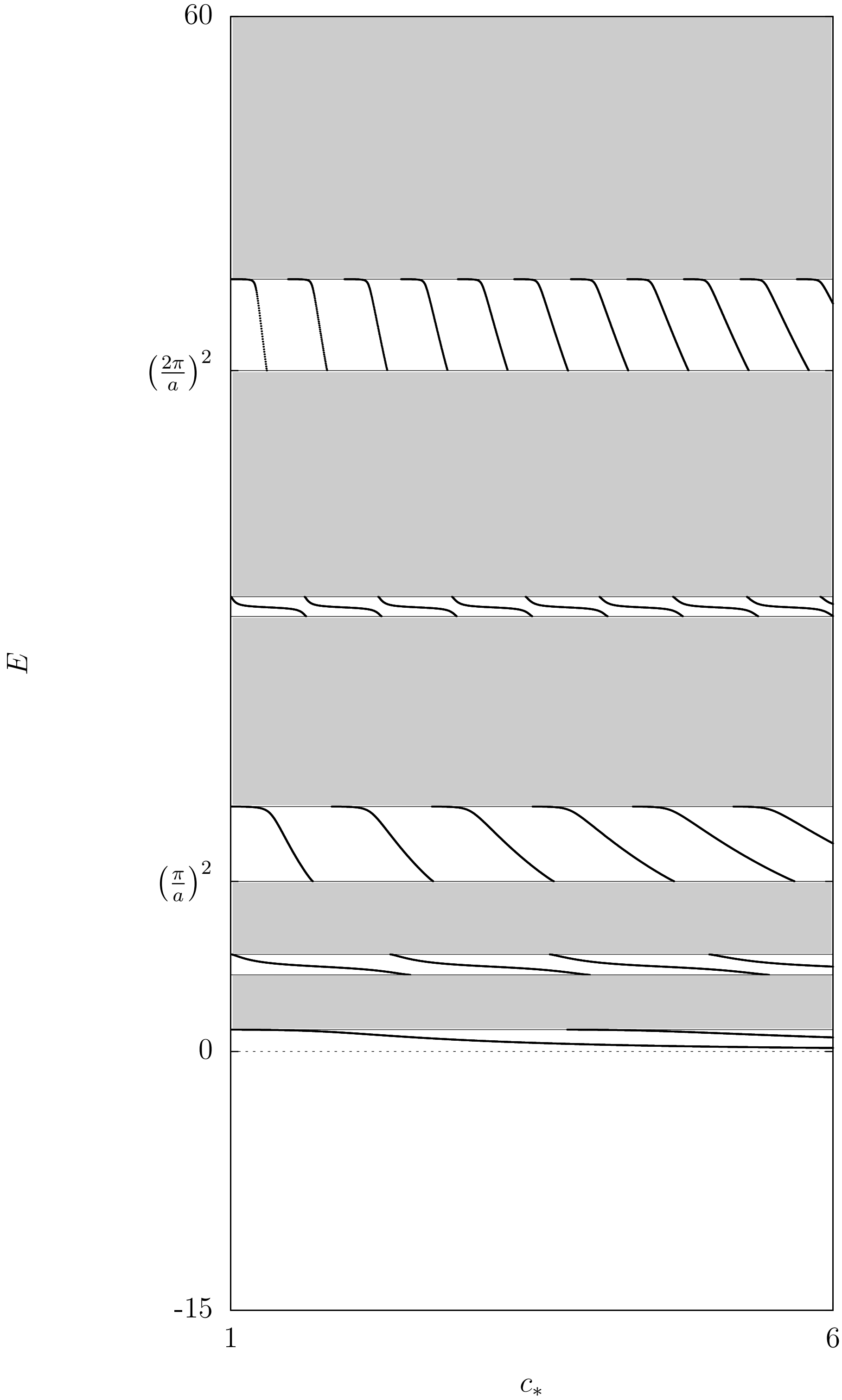

Figure 4.5: Trajectories of eigenvalues arising in spectral gaps as a result of increasing the length c_* of a selected tooth. Parameters $\beta = 1$, $\gamma = 0.5$, $\delta = 1$; c_* ranging from 1 to 6.

combination with the fact that $\lim_{\kappa\to\infty} \tilde{B}_*(\kappa) = +\infty$ implies that the graph of $\tilde{B}_*(.)$ intersects the graph of the right-hand side of (4.15) and hence, an eigenvalue is present below the lowest negative spectral band. The same holds even if there is no discontinuity of $\tilde{B}_*(.)$ in $(p, +\infty)$. Then we simply make use of the facts that

$$\tilde{B}_*(p) < \tilde{B}(p) = \tilde{B}(p) - \operatorname{sgn}(\tilde{B}(p))\sqrt{\tilde{B}^2(p) - 1},$$

following from (4.21), and $\lim_{\kappa\to\infty} \tilde{B}_*(\kappa) = +\infty$. Thus, the following statement holds:

Proposition 4.2.1: *Let $c_* > c$ and let the spectrum contain at least one negative spectral band. Then an eigenvalue exists below the lowest negative spectral band.*

This finding is illustrated in Figure 4.6, showing the behavior of the lowest eigenvalue found in the spectrum depicted in Figure 4.4.

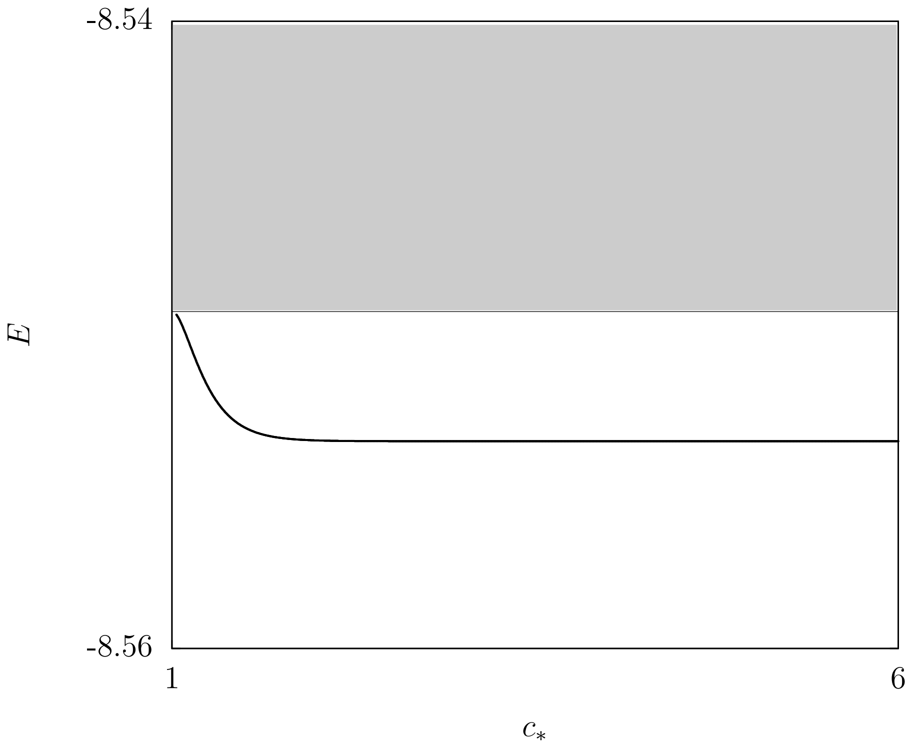

Figure 4.6: The lowest eigenvalue from Figure 4.4 enlarged.

4.3 Numerical results for local modifications of vertex conditions

In the previous section we explored the behavior of eigenvalues which arise after one of the teeth is prolonged. Here we make use of the general relations derived in Section 4.1 and show numerical results for spectra exposed to a modification of the vertex condition parameters at a selected vertex on the straight line.

The system is chosen to be the same as in the previous section, i.e. $a = 1$ and $c = 1$, and the same four combinations of the default vertex condition parameters β, γ, δ are considered.

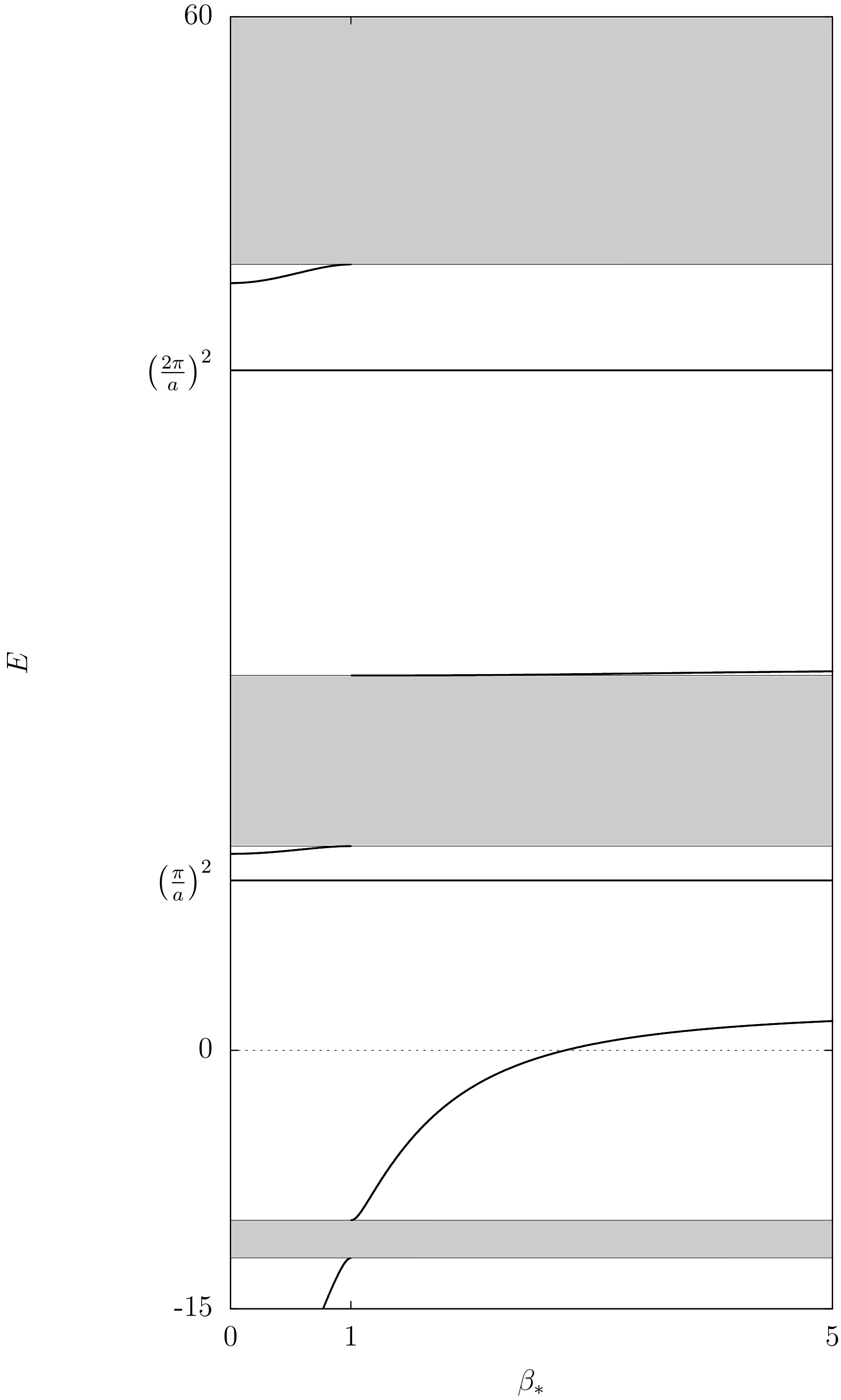

Figure 4.7: Trajectories of eigenvalues while changing β_* – one of the parameters determining the boundary conditions at a selected vertex on the line. Parameters $\beta = 1$, $\gamma = 0$, $\delta = -10$; β_* ranging from 0 to 5. Note the presence of degenerated spectral bands at $E = (\pi/a)^2$ and $E = (2\pi/a)^2$.

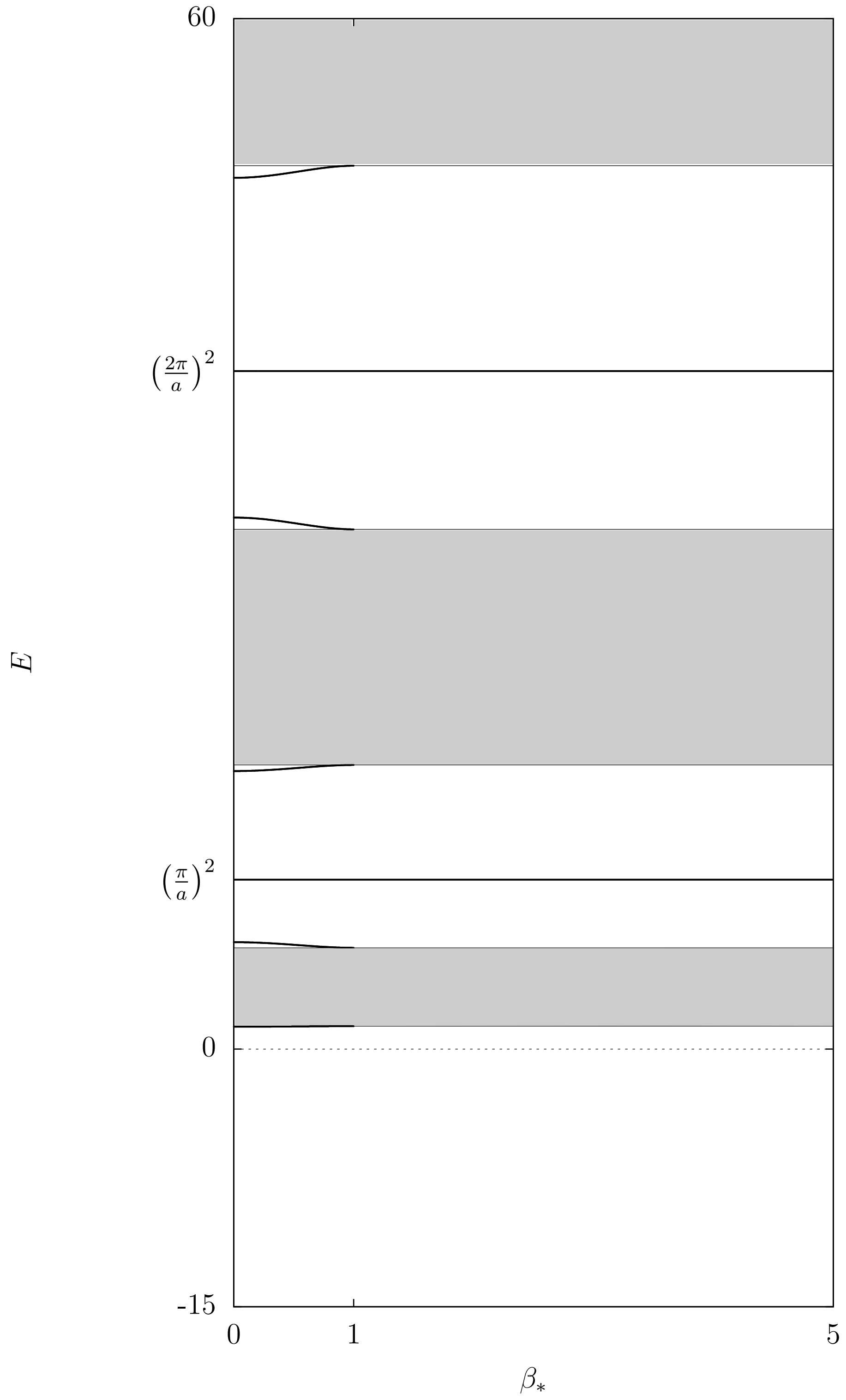

Figure 4.8: Trajectories of eigenvalues while changing β_* – one of the parameters determining the boundary conditions at a selected vertex on the line. Parameters $\beta = 1$, $\gamma = 0$, $\delta = 1$; β_* ranging from 0 to 5. Note the presence of degenerated spectral bands at $E = (\pi/a)^2$ and $E = (2\pi/a)^2$.

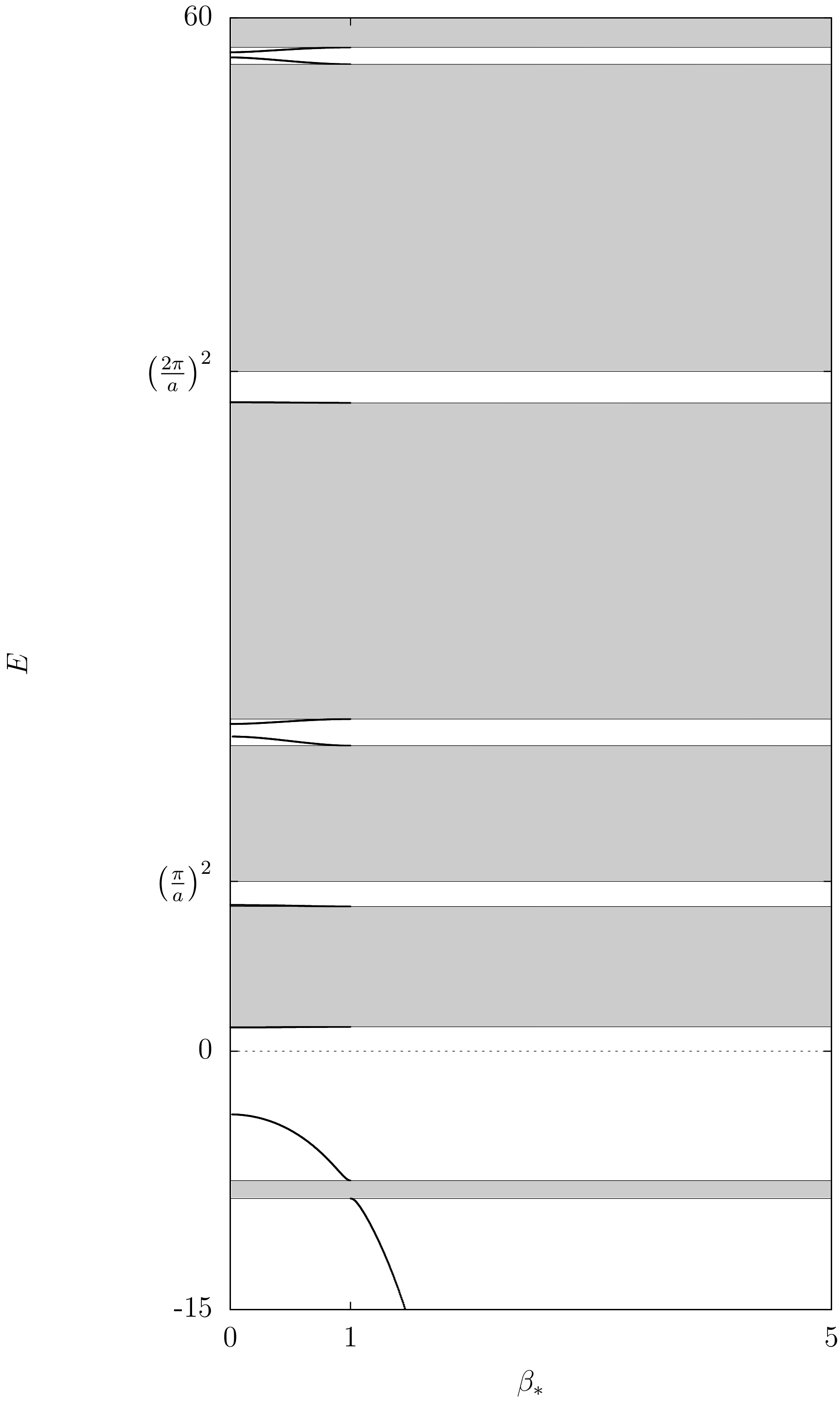

Figure 4.9: Trajectories of eigenvalues while changing β_* – one of the parameters determining the boundary conditions at a selected vertex on the line. Parameters $\beta = 1$, $\gamma = -0.5$, $\delta = 1$; β_* ranging from 0 to 5.

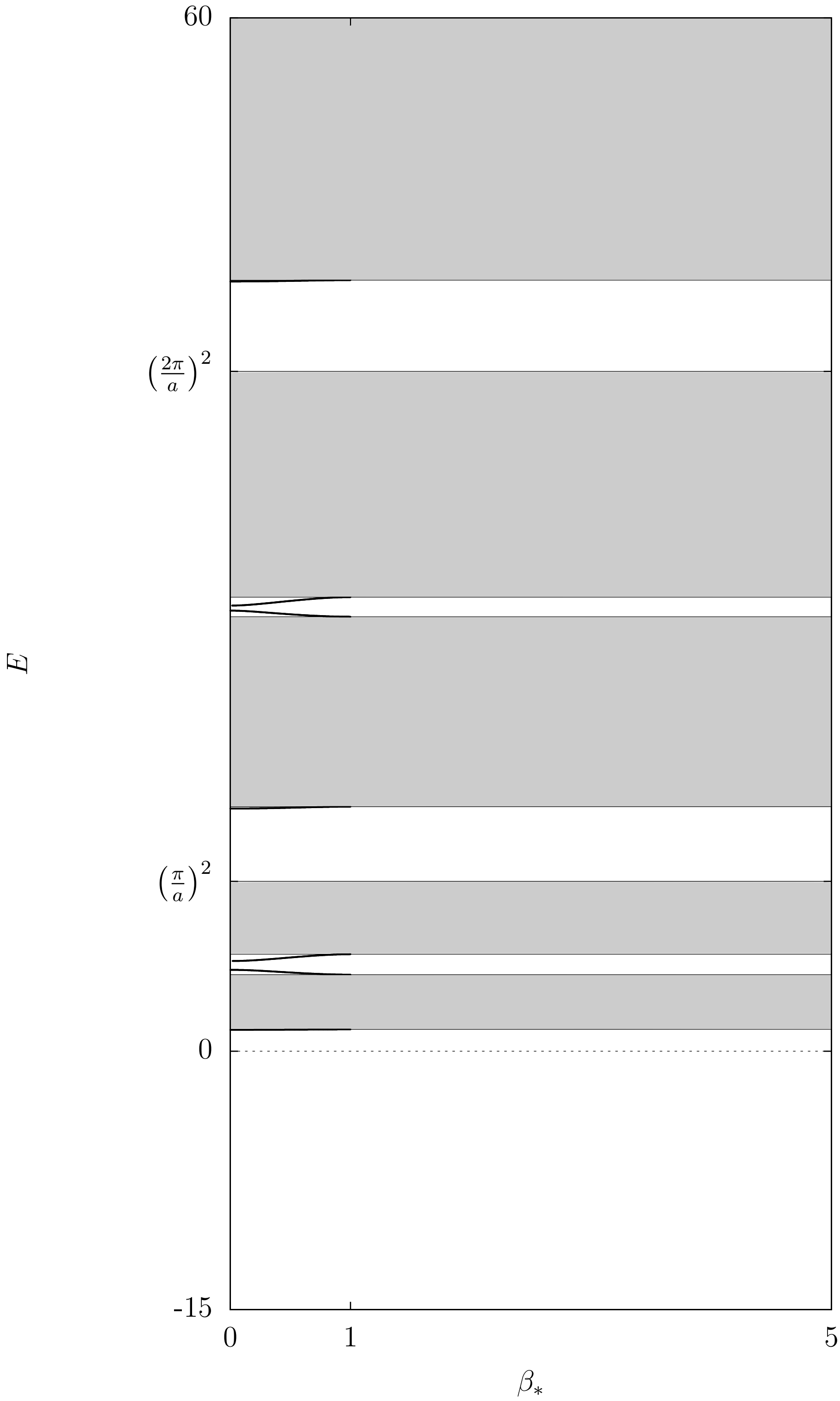

Figure 4.10: Trajectories of eigenvalues while changing β_* – one of the parameters determining the boundary conditions at a selected vertex on the line. Parameters $\beta = 1$, $\gamma = 0.5$, $\delta = 1$; β_* ranging from 0 to 5.

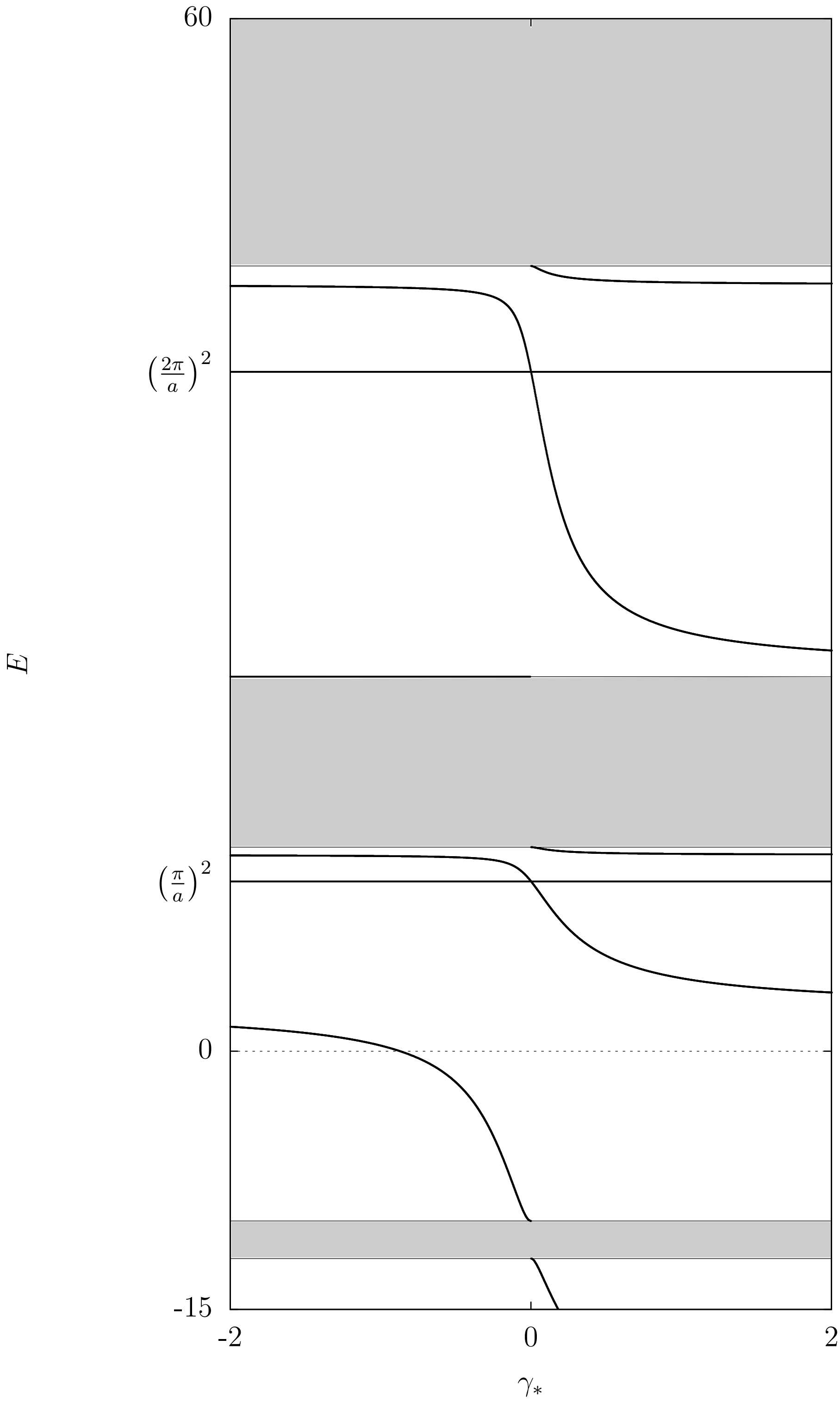

Figure 4.11: Trajectories of eigenvalues while changing γ_* – one of the parameters determining the boundary conditions at a selected vertex on the line. Parameters $\beta = 1$, $\gamma = 0$, $\delta = -10$; γ_* ranging from -2 to 2. Note the presence of degenerated spectral bands at $E = (\pi/a)^2$ and $E = (2\pi/a)^2$.

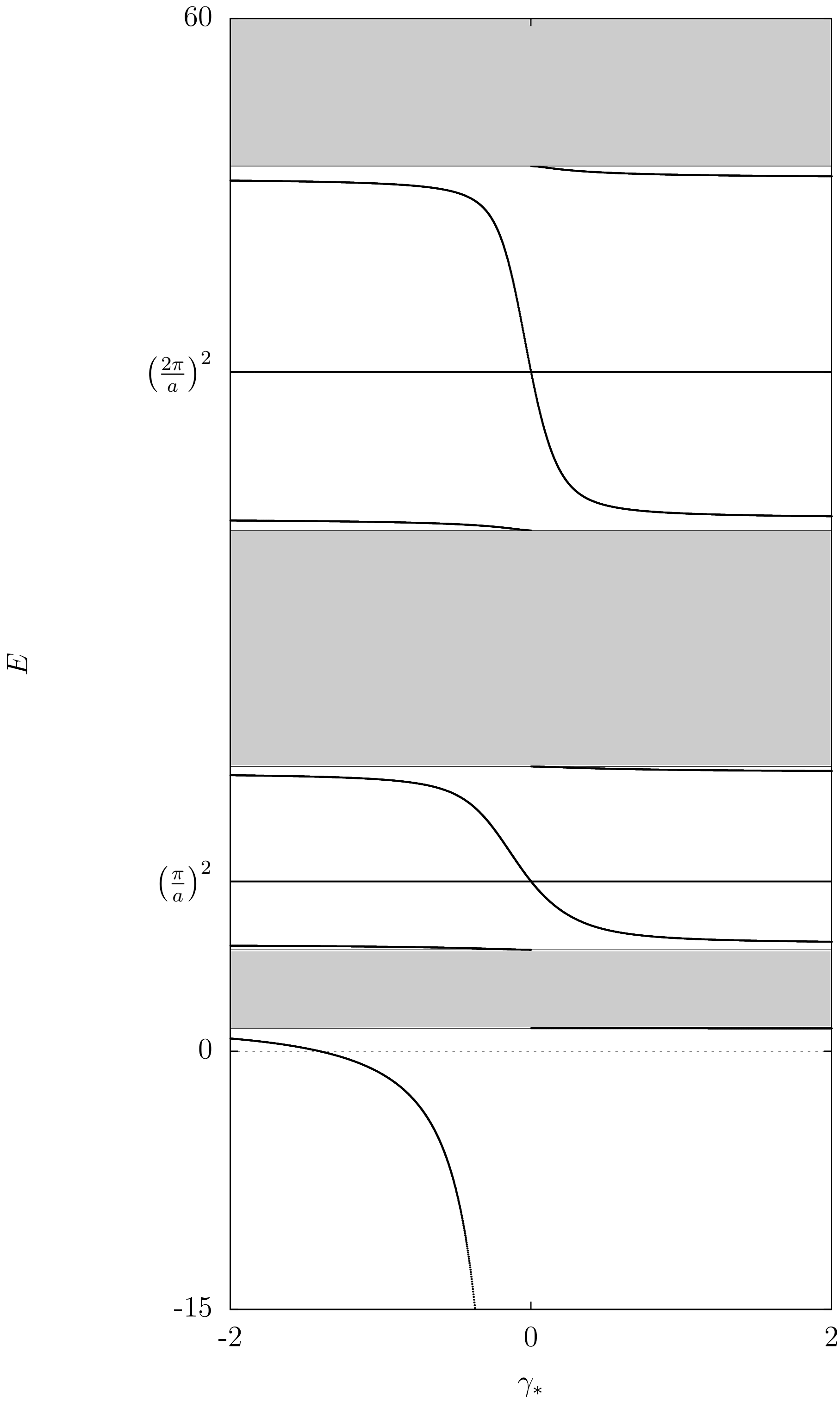

Figure 4.12: Trajectories of eigenvalues while changing γ_* – one of the parameters determining the boundary conditions at a selected vertex on the line. Parameters $\beta = 1$, $\gamma = 0$, $\delta = 1$; γ_* ranging from -2 to 2. Note the presence of degenerated spectral bands at $E = (\pi/a)^2$ and $E = (2\pi/a)^2$.

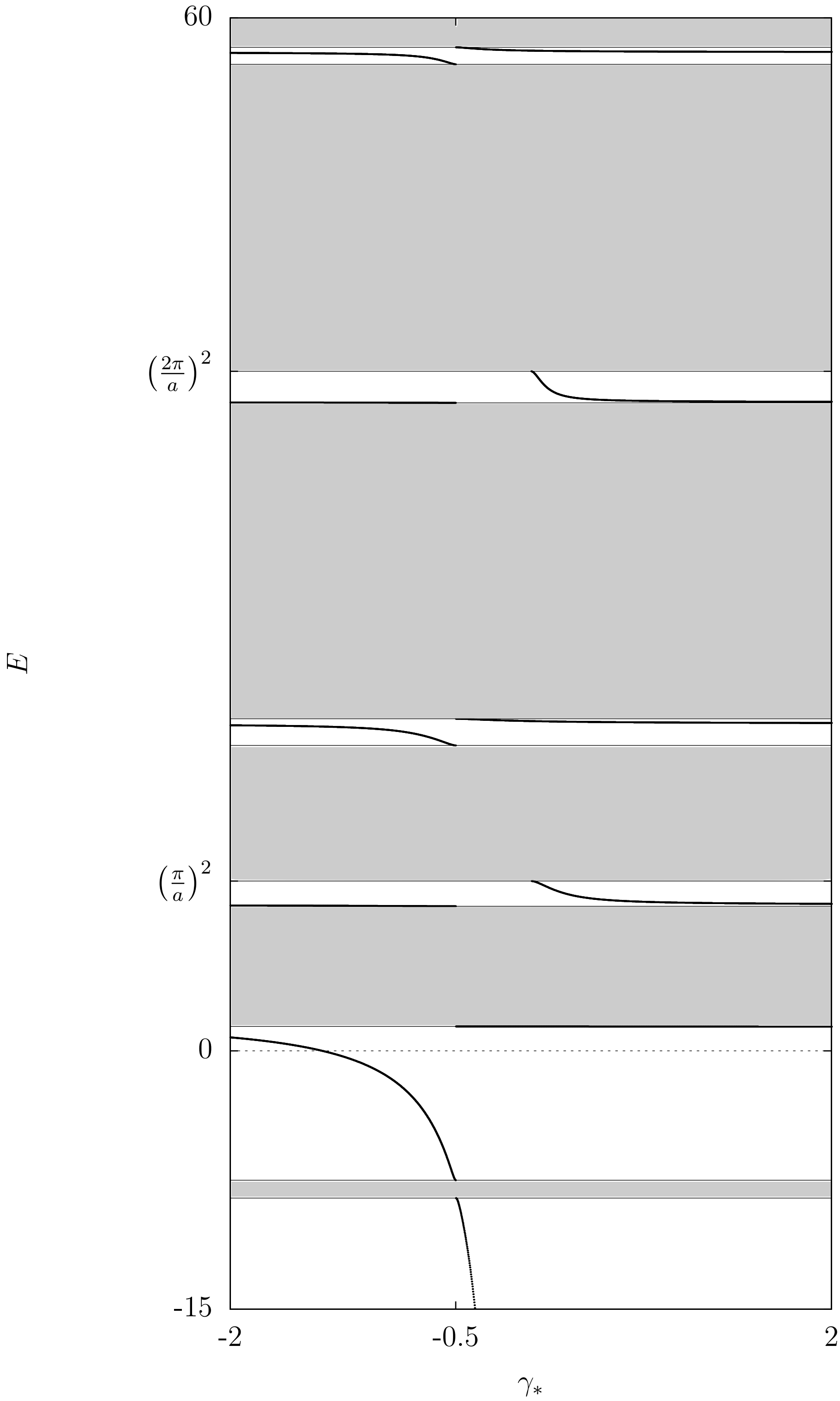

Figure 4.13: Trajectories of eigenvalues while changing γ_* – one of the parameters determining the boundary conditions at a selected vertex on the line. Parameters $\beta = 1$, $\gamma = -0.5$, $\delta = 1$; γ_* ranging from -2 to 2.

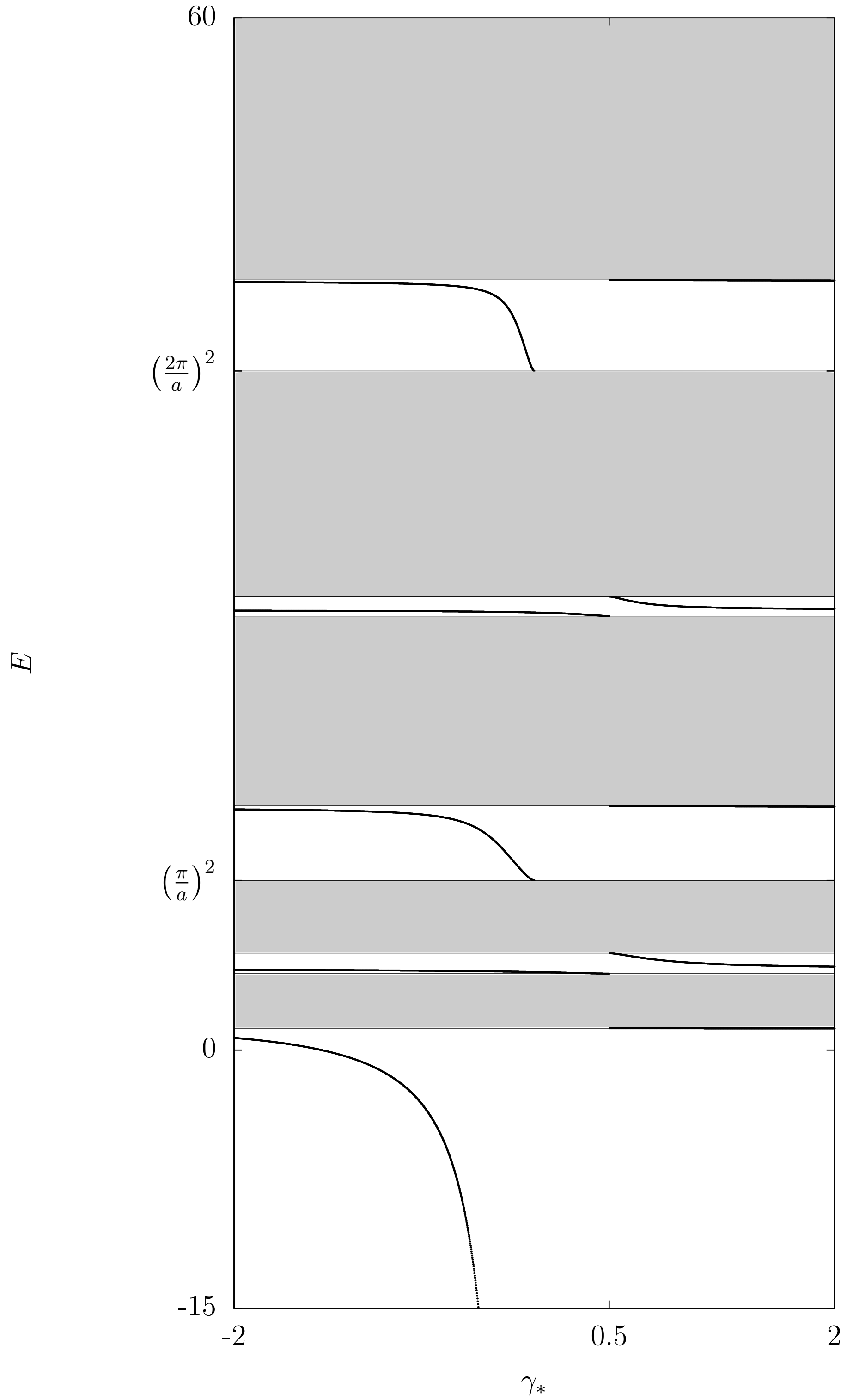

Figure 4.14: Trajectories of eigenvalues while changing γ_* – one of the parameters determining the boundary conditions at a selected vertex on the line. Parameters $\beta = 1$, $\gamma = 0.5$, $\delta = 1$; γ_* ranging from -2 to 2.

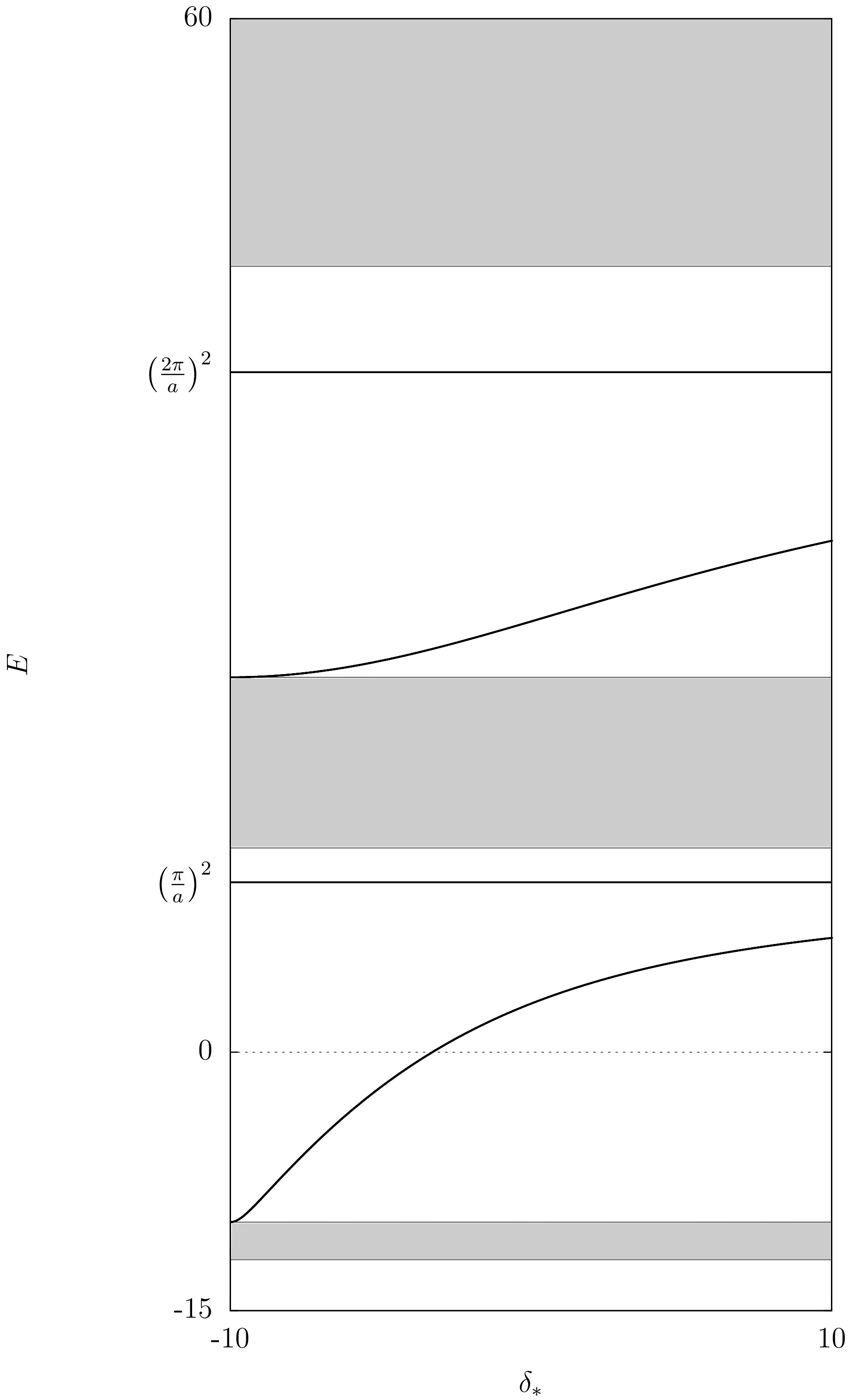

Figure 4.15: Trajectories of eigenvalues while changing δ_* – one of the parameters determining the boundary conditions at a selected vertex on the line. Parameters $\beta = 1$, $\gamma = 0$, $\delta = -10$; δ_* ranging from -10 to 10. Note the presence of degenerated spectral bands at $E = (\pi/a)^2$ and $E = (2\pi/a)^2$.

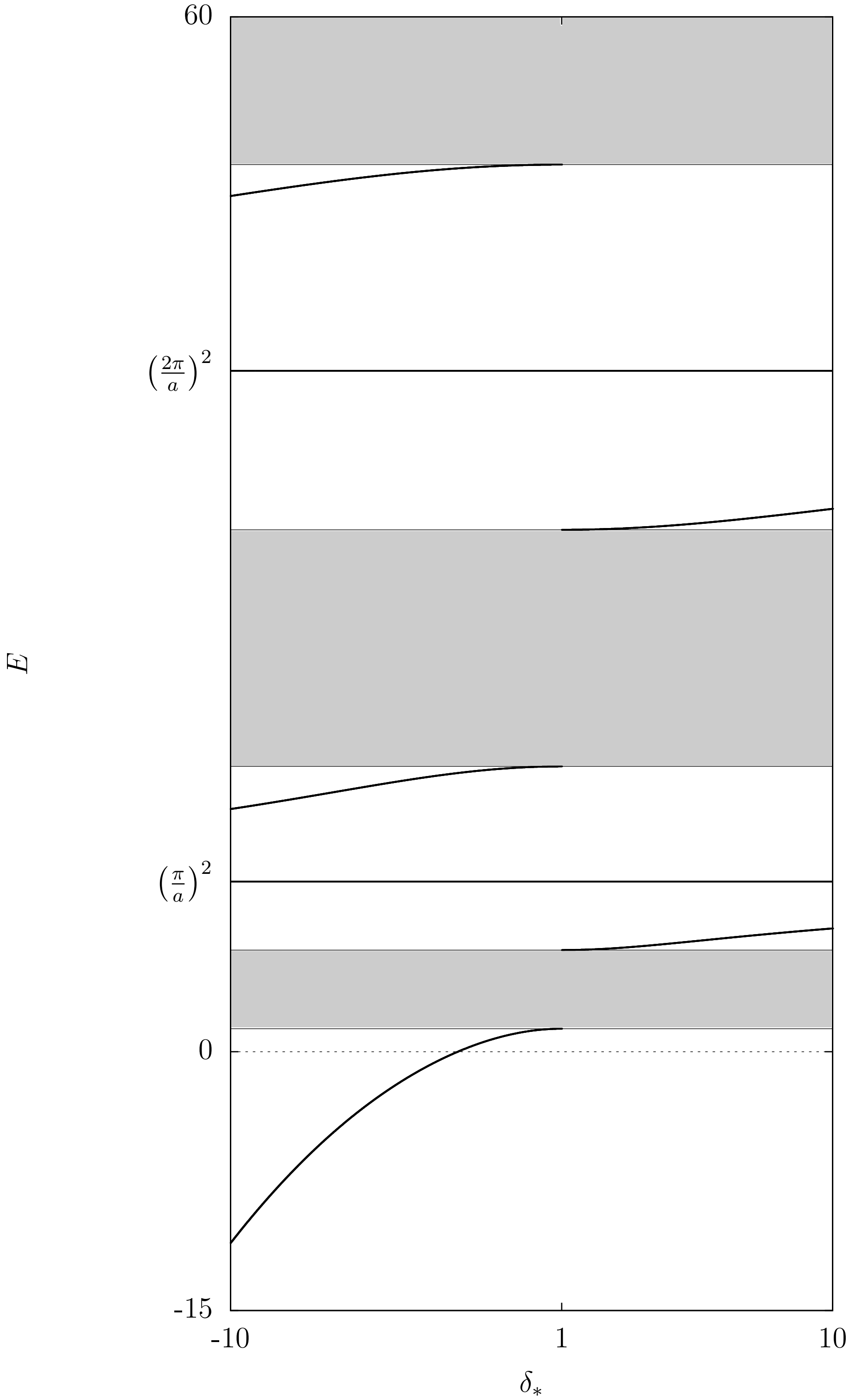

Figure 4.16: Trajectories of eigenvalues while changing δ_* – one of the parameters determining the boundary conditions at a selected vertex on the line. Parameters $\beta = 1$, $\gamma = 0$, $\delta = 1$; δ_* ranging from -10 to 10. Note the presence of degenerated spectral bands at $E = (\pi/a)^2$ and $E = (2\pi/a)^2$.

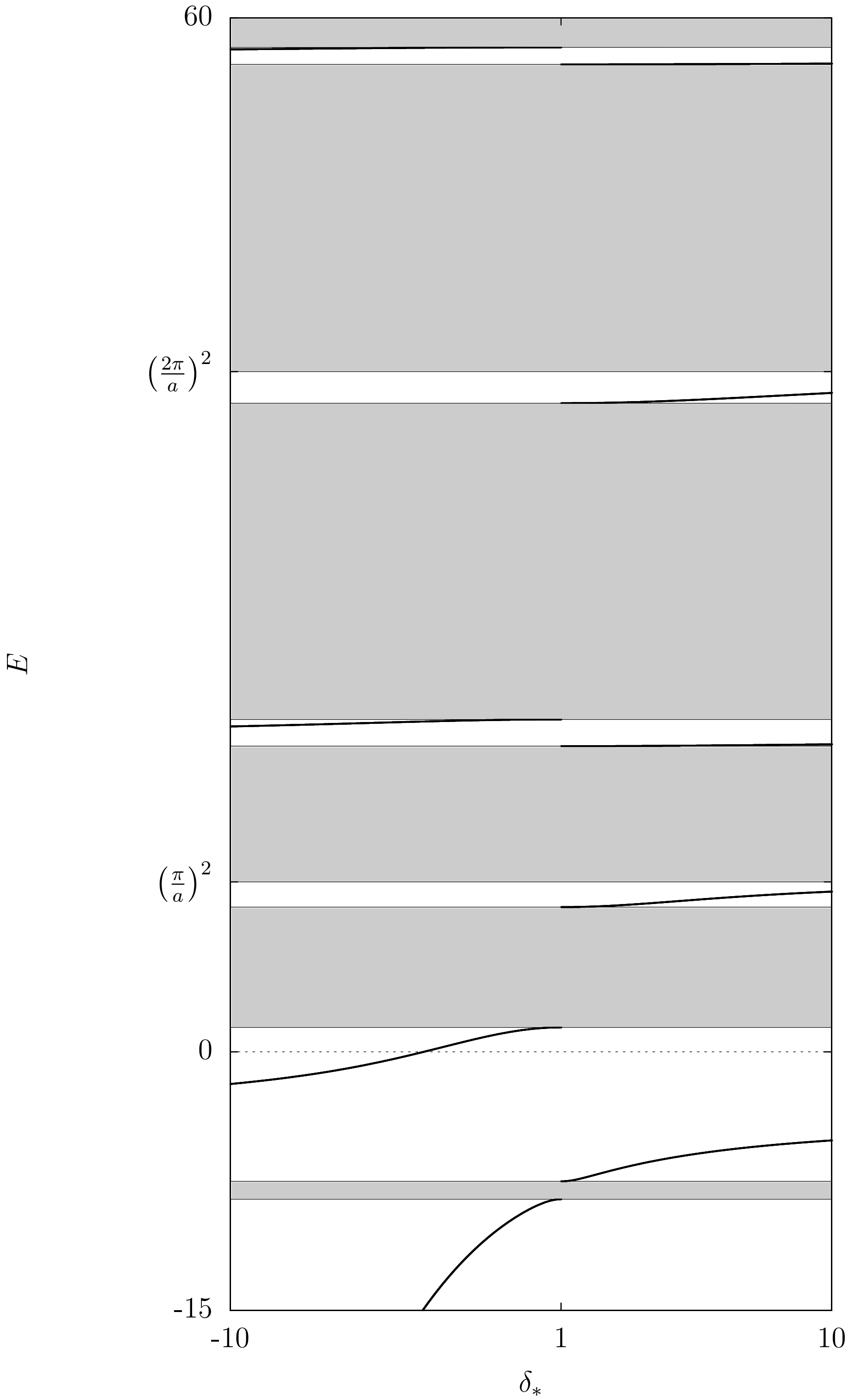

Figure 4.17: Trajectories of eigenvalues while changing δ_* – one of the parameters determining the boundary conditions at a selected vertex on the line. Parameters $\beta = 1$, $\gamma = -0.5$, $\delta = 1$; δ_* ranging from -10 to 10.

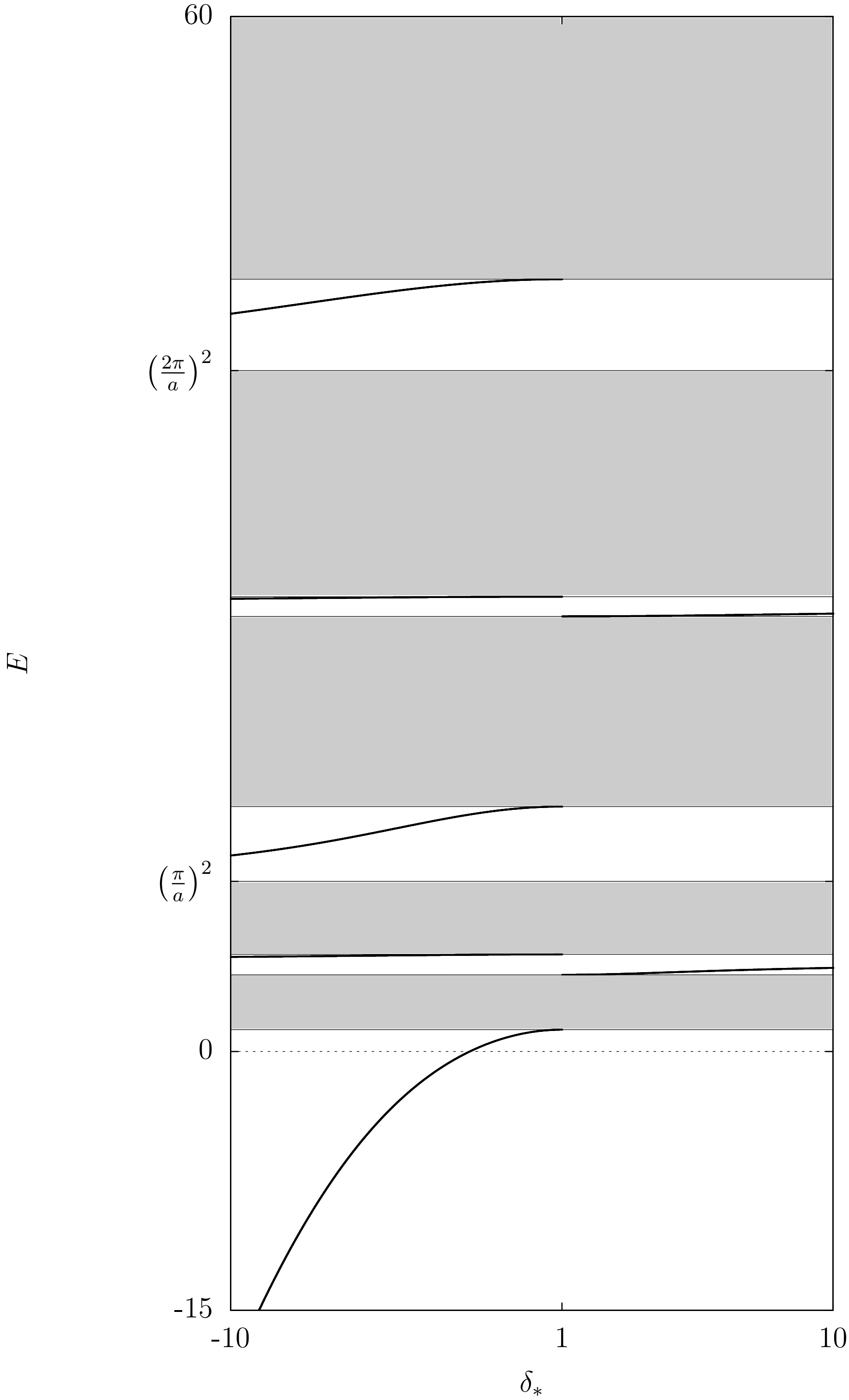

Figure 4.18: Trajectories of eigenvalues while changing δ_* – one of the parameters determining the boundary conditions at a selected vertex on the line. Parameters $\beta = 1$, $\gamma = 0.5$, $\delta = 1$; δ_* ranging from -10 to 10.

Chapter 5

Conclusion

In the preceding chapters we showed that the spectrum of the Hamiltonian associated with the infinite comb significantly depends on the geometry of the graph as well as the choice of vertex conditions. If a local perturbation is introduced, the newly arising eigenvalues exhibit interesting behavior.

Let us conclude by comparing our system with the bent chain graph studied in [DET08]. Both of these models have spectra containing an infinite number of spectral bands. Unlike in the chain, we do not find eigenvalues incorporated into the edges of positive spectral bands in our model. On the other hand, eigenvalues formed by degenerated bands can appear in our spectra.

The eigenvalues arising when a single tooth of the comb is prolonged behave differently from those appearing when the chain is bent. While in the case of the bent chain there is at least one and at most two eigenvalues in each spectral gap closure, in the case of the comb we can find spectra containing gaps with no eigenvalues at all for certain lengths of the prolonged tooth. Furthermore, the number of eigenvalues in each gap is not bounded from above if one increases the length of the tooth to infinity. Another difference is the fact that the eigenvalue trajectories observed in our numerical results are monotonically decreasing with respect to the length of the prolonged tooth, which contrasts with the non-monotonic dependence of eigenvalue positions on the bending angle in the chain. In our model, we can prove the monotonicity of eigenvalues located below the essential spectrum by using the technique of Dirichlet-Neumann bracketing, described in [RS78].

Finally, as follows from the spectra shown in Section 4.3, local modifications of vertex conditions result in substantially different behavior of eigenvalues in the gaps, and are surely worth a further investigation.

Bibliography

[AGHH04] S. Albeverio, F. Gesztesy, R. Høegh-Krohn, and H. Holden. *Solvable Models in Quantum Mechanics: Second Edition with an Appendix by Pavel Exner*. AMS Chelsea Publishing, 2004.

[BEH08] J. Blank, P. Exner, and M. Havlíček. *Hilbert Space Operators in Quantum Physics*. Springer, 2nd edition, 2008.

[CET10] T. Cheon, P. Exner, and O. Turek. Approximation of a general singular vertex coupling in quantum graphs. *Ann. Phys.*, 325:548–578, 2010.

[DET08] P. Duclos, P. Exner, and O. Turek. On the spectrum of a bent chain graph. *J. Phys. A: Math. Theor.*, 41(415206), 2008.

[EKW10] P. Exner, P. Kuchment, and B. Winn. On the location of spectral edges in Z-periodic media. *J. Phys. A: Math. Theor.*, 43(474022), 2010.

[EŠerešová94] P. Exner and E. Šerešová. Appendix resonances on a simple graph. *J. Phys. A: Math. Theor.*, 27:8269–8278, 1994.

[KS99] V. Kostrykin and R. Schrader. Kirchhoff's rule for quantum wires. *J. Phys. A: Math. Theor.*, 32:595–630, 1999.

[Kuc02] P. Kuchment. Graph models of wave propagation in thin structures. *Waves in Random media*, 12:R1–R24, 2002.

[Kuc04] P. Kuchment. Quantum graphs I. Some basic structures. *Waves in Random media*, 14:S107–S128, 2004.

[Kuc08] P. Kuchment. Quantum graphs: an introduction and a brief survey. In *Analysis on Graphs and its Applications*, Proc. Symp. Pure. Math., pages 291–405. AMS, 2008.

[RS78] M. Reed and B. Simon. *Methods of Modern Mathematical Physics IV: Analysis of Operators*. Academic Press, 1st edition, 1978.